The end of the Cretaceous: depositional palaeogeographical reconstruction of the Gulf of Mexico and adjacent areas just prior to the Chicxulub impact

John William Snedden[1]*, Christopher M. Lowery[1] and Timothy F. Lawton[2]

[1]Institute for Geophysics, The University of Texas at Austin, 10100 Burnet Road (R2200), Austin, TX 78758-4445, USA

[2]Bureau of Economic Geology, Jackson School of Geosciences, The University of Texas, 10100 Burnet Road (R2200), Austin, TX 78758-4445, USA

JWS, 0000-0002-7450-2666

*Correspondence: jsnedden@ig.utexas.edu

Abstract: Until recently, information about the end of the Cretaceous was based upon investigation of global outcrop sections. New subsurface drilling and characterization from well cores and logs in the Gulf of Mexico Basin have greatly illuminated the end Cretaceous event. However, the palaeogeography of the late Maastrichtian just prior to bolide impact is less well understood and is of great importance in terms of modelling the resulting distribution and composition of the Chicxulub impact material, as well as tsunami and seiche wave height. Here, we examine the Maastrichtian strata in the basin, synthesizing lithostratigraphy and chronostratigraphy, tectonic plate reconstructions, global and local sea level history, palaeoclimate and depositional systems. Our new Maastrichtian palaeogeographical reconstruction shows the basin prior to the Chicxulub impact at a time of globally high sea level, with widespread deposition of deepwater chalks and shallow marine carbonates and local siliciclastic shorelines fed by the nascent Cordilleran belt. Stratigraphic correlations of wells and outcrops illustrate the range of palaeoenvironments from coastal plain to deep marine. As much as 610 m (2000 ft) of Maastrichtian and Campanian section is mapped around the basin, reflecting accommodation provided by basin subsidence, salt deflation and palaeophysiography. A large thickness of carbonates accumulated in the basin centre, with steep shoreline to basin gradients particularly in Mexico. At the end of the Cretaceous, carbonate palaeoenvironments probably covered 96% of the Gulf of Mexico Basin, with less than 4% of the area likely occupied by siliciclastic systems, a distribution that evolved from the Early Cretaceous. Our maps thus explain dominance of carbonate breccia and chalks in K–Pg boundary units deposited over the basin sites proximal or distal to the Chicxulub impact crater. This also elucidates the large impedance contrast and high amplitude seismic response of the K–Pg boundary horizon, mappable over vast portions of the basin.

Palaeogeographical reconstructions have long been used for scientific purposes and economic applications. The distribution of past terrestrial and marine environments is a result of tectonic, eustatic, climatic and hydrologic processes that evolved over geological time to form our present-day global biosphere, landscape and seascape. Exploration for mineral resources and potential sites for storage of anthropogenic carbon are also better informed when conducted within a palaeogeographical context.

The Cretaceous system, first defined 200 years ago by Jean d'Omalius d'Halloy from outcrops in Europe, represents the pinnacle of many trends of the Mesozoic Era, and its termination starts the transition to the more familiar world of the Cenozoic Era. Like all major divisions of geological time, the transition between the Mesozoic and the Cenozoic is based upon the large number of extinctions of terrestrial and marine fauna and flora which, with increasing study, were eventually recognized to be geologically rapid (e.g. Luterbacher and Premoli Silva 1964; Percival and Fischer 1977; Romein 1977; Thierstein and Okada 1979). With the discovery of an iridium anomaly coincident with these extinctions in 1980 (Alvarez *et al.* 1980; Smit and Hertogen 1980), a growing consensus emerged that the Mesozoic was terminated by a bolide impact. This culminated in the discovery of the Chicxulub crater in 1991 on the Yucatan carbonate platform in the Gulf of Mexico. After reexamination of old gravity anomaly surveys, Hildebrand *et al.* (1991) located a large circular anomaly first identified as a potential impact crater by Penfield and Carmargo-Zanoguera (1981). With examination of core samples from old Pemex exploration wells within the crater, they found shocked quartz and other impact debris of precisely the same age as the iridium anomaly in distal sites. In the last 40 years, a growing consensus emerged that an extraterrestrial object had impacted the Yucatan Platform in the Gulf of Mexico, ending the Maastrichtian Stage (Schulte *et al.* 2010; Morgan *et al.* 2017). The multitude of

From: Hart, M. B., Batenburg, S. J., Huber, B. T., Price, G. D., Thibault, N., Wagreich, M. and Walaszczyk, I. (eds) *Cretaceous Project 200 Volume 2: Regional Studies*. Geological Society, London, Special Publications, **545**, https://doi.org/10.1144/SP545-2023-51

papers about this impact and the resulting extinction that have been written are far too numerous to begin to summarize here. Key review papers for the interested reader include Claeys *et al.* 2002; Schulte *et al.* (2010) (still the best review of the impact hypothesis); Lowery *et al.* (2019) (a review of impact processes); Gulick *et al.* (2019) (a review of physical processes associated with the impact in the Gulf of Mexico); and Hull *et al.* (2020) (a comprehensive review of impact-related climate change).

However, this accelerating avalanche of K–Pg research tends to focus on the impact event itself. The palaeogeography and lithological substrate of the late Maastrichtian are also less well-documented than the post-impact strata (and recovery of fauna and flora) yet remain important in terms of modelling the resulting distribution and composition of the Chicxulub impact products. The purpose of this paper is to introduce a depositional palaeogeographical reconstruction of the late Maastrichtian in the Gulf of Mexico Basin just prior to the Chicxulub impact event. Erosion and disturbance of the uppermost Maastrichtian by the impact-related physical processes obviously present a challenge in reconstructing this depositional palaeogeography. Reporting on the end of the Cretaceous is thus an appropriate 'book end' for this special volume celebrating the 200th anniversary of the founding of the Cretaceous.

Previous work

Prior palaeogeographical reconstructions of the Gulf of Mexico Basin vary considerably in type and coverage. Early reconstructions of the form and extent of past land- and seascapes were limited by relatively poor exposures in the Gulf Coastal Plain (e.g. Schuchert 1955), particularly for sandstones and mudstone-dominated sections which weathered more readily than Mesozoic carbonates. While later reconstructions (reported in multiple chapters of Salvador 1991) made use of (but did not report on) subsurface exploration wells that retrieved cuttings, cores and petrophysical logs of lithology, many more industry wells have been drilled. Combined with new seismic reflection and refraction surveys and novel gravity/magnetic data, workers have better delineated deep crustal types, depositional basins and structural highs (e.g. Van Avendonk *et al.* 2015; Pindell *et al.* 2016; Filina and Beutel 2022). Plate tectonic models of the Maastrichtian generally resemble the present-day basin configuration, as the Yucatan (Maya) block had rotated to its present position by the Late Jurassic (Salvador 1991; Filina *et al.* 2021).

Global maps depicting the position of palaeocoastlines, land masses and ocean basins have been greatly improved by combining plate tectonic models with digital elevation models (DEM) of palaeotopography and palaeobathymetry (Kocsis and Scotese 2021). Calibrated against spatial distribution of environment specific fossils, these depict variations due to continental flooding or subaerial exposure related to eustasy, structural uplift, subsidence and palaeoclimate trends. For the time interval of interest here, two extrabasinal elements are most important to consider: (1) evolution of the Western Interior Seaway (WIS); and (2) presence of an equatorial marine strait between North and South America (Central American Seaway). Recent global palaeogeographical reconstructions depict a WIS directly connected to the Gulf of Mexico at 80 Ma (Campanian; Fig. 1a; Scotese 2021) but one that had withdrawn to the north by 66 Ma (Fig. 1b; Scotese 2021). These reconstructions also show the Central American Seaway between North and South America open until the Miocene when the Isthmus of Panama land bridge began to develop (Coates *et al.* 1992; Montes *et al.* 2015; O'Dea *et al.* 2016). Numerical models of the end Cretaceous event indicate that this open passage also permitted propagation of tsunami waves into the southwestern Pacific (Range *et al.* 2022).

Palaeogeographical reconstructions at a global scale are important for understanding the connection of the Gulf of Mexico Basin to seaways and ocean basins. Our more Gulf of Mexico Basin-focused depositional reconstruction of the Maastrichtian will provide additional detail and more regional to local granularity to fully illuminate the end Cretaceous depositional palaeogeography. This hopefully will serve as a useful baseline for future studies of the K–Pg impact processes and products. We also report on new deep basin wells that illuminate the basin centre, complementing basin margin outcrop studies (Lawton *et al.* 2020). Subsequent sections of this paper synthesize information on the Gulf of Mexico depositional systems, chrono- and lithostratigraphy, eustasy, tectonic processes and palaeoclimate that support our depositional palaeogeography maps.

Methods of reconstruction

Reconstructing the depositional palaeogeography of the Maastrichtian of the Gulf of Mexico is challenging, given its age (72–66 Ma), overprint of later tectonic events (such as the early Cenozoic Laramide orogeny and Miocene Appalachian rejuvenation) and limited outcrop exposures in the US Gulf Coastal Plain (Fig. 2; Boettcher and Milliken 1994; Jackson *et al.* 2011). Thus, a comprehensive understanding of this phase of basin depositional history involves detailed analysis of subsurface wells and reflection seismic data. Well-based thickness maps of the gross interval, sandstone- and carbonate-

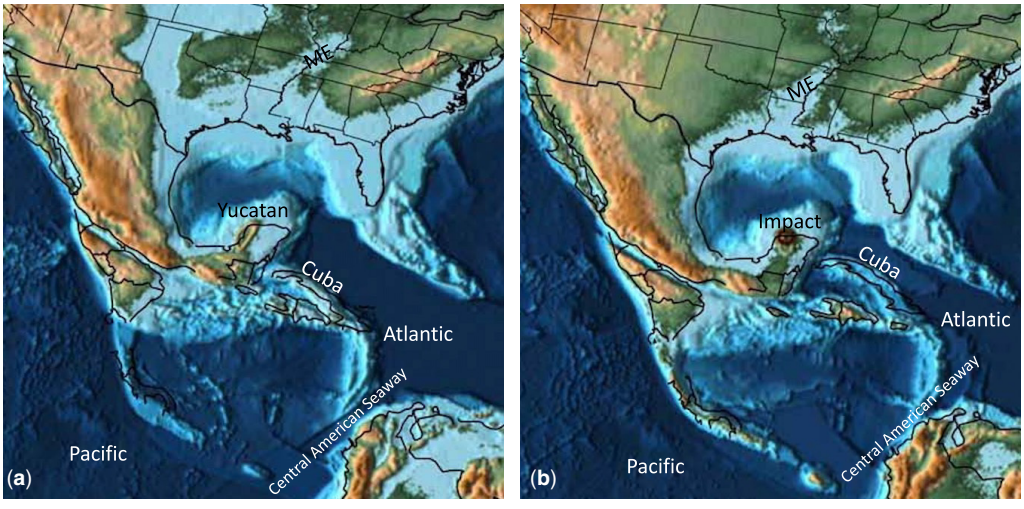

Fig. 1. Palaeoglobe (Mollweide projection) maps for (**a**) Campanian (80 Ma) and (**b**) K–Pg boundary (66 Ma). Source: slightly modified from Scotese (2021).

bearing sections help delineate regional sandstone depocentres, which can be linked to palaeorivers or carbonate platform margins and grainstone banks. Structure contour maps based on basin-scale seismic mapping assist in defining pre-existing basement highs and basinal embayments, the latter often acting as sites of enhanced accommodation. At the larger basin-scale, palaeogeographical reconstructions are

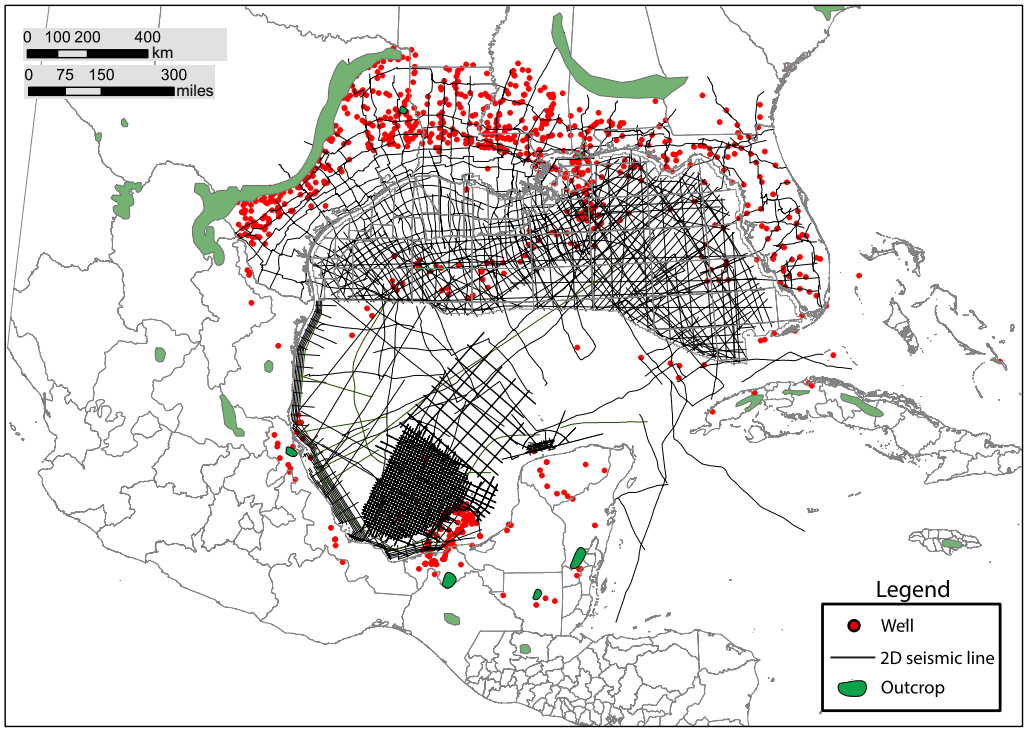

Fig. 2. Gulf of Mexico Basin study area and database map. Source: Maastrichtian outcrop locations from Schuchert (1955), Kornecki *et al.* (2017) and localities discussed in the text.

informed by plate tectonic restorations, synthesis of literature, interpretation of depositional environments and palaeotransport processes.

Database

Studies of Maastrichtian strata in North America are mostly based on widespread outcrops in the Cretaceous WIS (Pyles and Slatt 2000; Carvajal and Steel 2006) and Mexico (Lawton *et al.* 2020), but relatively limited exposures in the US Gulf Coastal Plain (Fig. 2; e.g. Pessagno 1969; Pessagno *et al.* 2023). For our palaeogeographical reconstructions in the Gulf Coastal Plain and basin, we supplement local outcrop work (e.g. Snedden 1991; Smit *et al.* 1996; Lawton *et al.* 2021) with a robust subsurface database of wells and recent vintage reflection seismic data (Fig. 2). The Gulf of Mexico Basin, which includes onshore, nearshore and deepwater tranches, has been the site of active drilling since the 1900s. For the United States portion of the basin, information such as logs from onshore and state waters is available from state surveys such as the Bureau of Economy Geology (BEG) at the University of Texas (https://www.beg.utexas.edu/about/facilities/geophysical-log-facility). For offshore federal waters, one can procure logs and ancillary data from the Bureau of Safety and Environmental Enforcement Data Centre (https://www.data.bsee.gov/).

The recent opening of Mexico to international exploration has yielded both proprietary and public information on the southern Gulf of Mexico, closer to the Chicxulub impact site. Our offshore database here primarily consists of one publicly available older (1970–80s) 2D seismic survey collected by The University of Texas Institute for Geophysics in Mexico and adjacent areas of the USA, which is available for download at the Academic Seismic Portal (https://www.marine-geo.org/collections/#!/collection/Seismic%23summary#summary). More recently acquired 2D seismic surveys in offshore Mexico from Multiclient Geophysical, ION-TGS, PGS and Searcher remain proprietary. However, we provide several maps derived from these seismic data supporting our interpretations. Well data in Mexico are not released publicly, though useful information from wells used in university theses and dissertations is public and accessible at sites like that of the Universidad Nacional Autónoma de México (known by its Spanish acronym, UNAM; https://www.unam.mx). Other Mexico well information including well logs comes from published papers and annual reports of Pemex, which are released to the public near year end.

Lithostratigraphy and chronostratigraphy

As mentioned, the Maastrichtian and immediately overlying Danian section of the Gulf of Mexico are known from both outcrops and subsurface well penetrations. For over 100 years, exploration and producing wells have drilled through these intervals on the way to deeper objectives in the Cretaceous and Jurassic. Early stratigraphic correlations using megafossils and well logs produced a rather provincial nomenclature based largely on lithology, thus a lithostratigraphic system with limited age control. Improvements were made using benthic foraminifera, but these are substrate sensitive and less useful for precise age control in some cases. The first comprehensive stratigraphic chart of the Gulf of Mexico assembled by Salvador (1991) reflects this lithostratigraphic correlation system. Within the Maastrichtian, more than 20 different formation and member names are used (Fig. 3). More recent palynological investigations of Maastrichtian outcrops yielded only small numbers of age diagnostic taxa (Mahmoud 2004), but these proved to be helpful for palaeoenvironmental

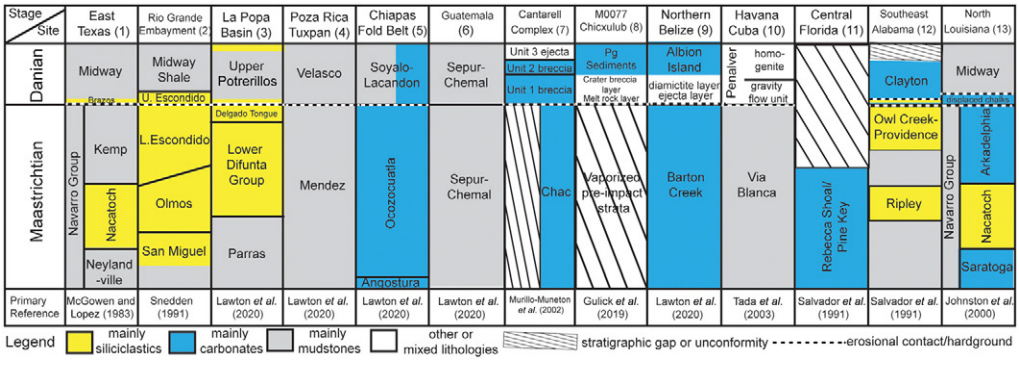

Fig. 3. Lithostratigraphic sections around the Gulf of Mexico. For outcrop and well locations, see Figure 4.

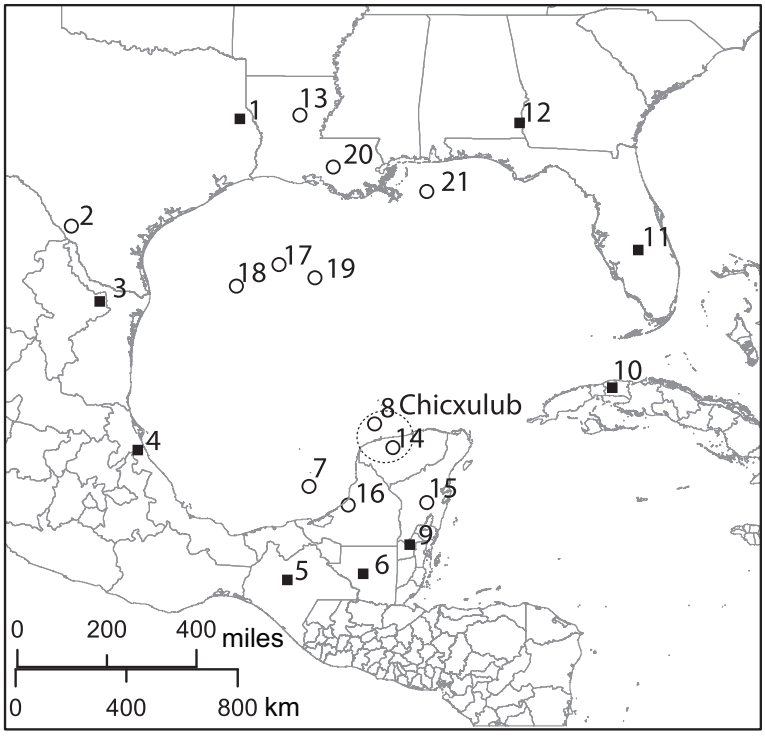

Fig. 4. Location of sections for outcrop and wells sections of Figure 3 and Table 2. Outcrops are indicated by black-filled squares and wells by white-filled circles. Dashed circle shows general location of the Chicxulub impact crater.

interpretations as discussed in later sections of this paper.

Recent major improvements in age control in the greater Gulf of Mexico Basin have come with the use of planktic foraminifers and calcareous nannofossils (Olson *et al.* 2015; Cunningham *et al.* 2022; Pessagno *et al.* 2023). These fossils are less sensitive to substrate conditions, have temporally short ranges in many cases and more global distributions. This is particularly important as the oil and gas industry moved into progressively deeper offshore waters where these faunal and floral forms are more abundant. Correlations to Mexico and areas to the south have been recently updated (Lawton *et al.* 2020), making use of first cycle volcanic zircons and U–Pb geothermochronology to provide the strata maximum depositional age, as well as provenance. While several Maastrichtian lithostratigraphical units remain less age-constrained, progress continues to be made (e.g. Ripley Sandstone; see Jackson *et al.* 2021).

Various biostratigraphic datums are useful to identifying the Danian section (including the K–Pg boundary unit) of the Gulf of Mexico and differentiating it from the underlying late Maastrichtian interval. Table 1 shows a selection of common faunal and floral markers useful for this purpose, but the reader is also referred to robust tabulations in other papers (e.g. Bralower *et al.* 1998; Arz *et al.* 2001, 2022; Denne *et al.* 2013; Leighton *et al.* 2017; Lowery *et al.* 2021; Rodríguez-Tovar *et al.* 2022; Pessagno *et al.* 2023). Lithostratigraphical nomenclature for the post-Maastrichtian section varies around the basin margin (Figs 3 & 4). In the Rio Grande basin of Texas (1200 km north of Chicxulub; location 2 of Figs 3 & 4), the Escondido Formation includes both the pre-impact Maastrichtian strata present at the outcrop (Cooper 1973) and post-impact products of the impact (Fig. 5; Kinsland and Snedden 2016; Snedden and Galloway 2019). While original analyses of planktic foraminifers from the lower Escondido Formation in nearby outcrops indicate assignment strictly to the Maastrichtian Stage (Cooper 1973; Snedden 1991), the presence of detrital zircon grains from the uppermost Escondido in a well in Webb County with a maximum depositional age of 66 Ma indicates the upper Escondido Formation is the K–Pg boundary deposit (Snedden *et al.* 2022). In La Popa Basin of northeastern Mexico (location 3 of Figs 3 & 4), ejecta-bearing conglomerate fills

Table 1. Non-exhaustive list of the occurrences of late Maastrichtian to early Danian planktic foraminiferal and calcareous nannoplankton zones across the Gulf of Mexico

Stage	Biozone (base)	Calibrated age (Ma)	Datum	Taxon	Gulf of Mexico sites
Danian	NP6	62.1	B	*Sphenolithus moriformis*	M0077[1]
	P3a	62.33	B	*Morozovella angulata*	M0077[2] DeSoto Canyon[3]
	P2	62.68	B	*Praemurica uncinata*	M0077[2] DeSoto Canyon[3] 95[4]
	NP4	63.15	Bc	*Toweius pertusus* (circular)	M0077[1]
	P1c	63.92	B	*Globanomalina compressa*	M0077[2] DeSoto Canyon[3] 95[4] Yaxcopoil-1[5] Lynn Creek[6] Braggs[6] Millers Ferry[7] La Ceiba[8]
	P1b	65.2	B	*Subbotina triloculinoides*	M0077[2] 95[4] Yaxcopoil-1[5] Marengo County[7] Moncada[9] La Ceiba[10]
	NP3	65.53	Bc	*Chiasmolithus danicus*	M0077[1]
	NP2	65.7	B	*Cruciplacoluthis tenuis*	M0077[1] Brazos – not observed but inferred based on occurrence of *Cruciplacolithus intermedius*[11]
	P1a	65.72	T	*Parvularugoglobigerina eugubina*	M0077[2] 95[4] Moncada[9] Millers Ferry[12] Bochil[13]
	Pα	66	B	*Parvularugoglobigerina eugubina*	M0077[14] 95[4] Moncada[9] Millers Ferry[12] Bochil[15] Guayal[15]
			B	Calcisphere acme (*Cervisiella* spp.)	M0077[1,2] Brazos[11] Mexican Fold Belt[16]
	P0/NP1	66.04	B	Survivor taxa*	M0077[14] 95[4] Moncada[9] Brazos[11] Bochil[15] Guayal[15]
		66.04	B	K–Pg boundary cocktail	M0077[14] 95[2,17] 536[17] 540[17] Bochil[15] Moncada[9] Guayal[15] Mexican Fold Belt[16] Alaminos Canyon 557[18] Keathley Canyon 596[18] Keathley Canyon 102[18]
Maastrichtian	P. hant.	66.39	B	*Plummerita hantkeninoides*	La Ceiba[10]
	P. haria.	67.64	B	*Pseudoguembelina hariaensis*†	Brazos[19]
	CC26	67.82	B	*Nephrolithus frequens*	Millers Ferry[12] Brazos[19]
	A. maya.	69.72	B	*Abathomphalus mayaroensis*	La Ceiba[10] Mendez Station[20] Fort Lincoln[20]
	R. fruc.	70.14	B	*Racemiguembelina fructicosa*	Lynn Creek[7] Moscow Landing[7] Shell Creek[7] Prairie Bluff Landing[7] Braggs[7] Mussel Creek[7] Limestone County[21] Milam County[21] Guayal[15]

B, Base; Bc, Base common; T, top.

*P0 is between the top of Cretaceous taxa and the base of *P. eugubina*; NP1 is between the Top Cretaceous taxa and the base of *C. tenuis*.

†Important to note that *Pseudoguembelina hariaensis* was erected by Nederbragt (1991) and so its occurrence wouldn't have been noted by earlier studies.

[1]Jones *et al.* (2019); [2]Lowery *et al.* (2021); [3]Kelly *et al.* (1996); [4]Lowery and Bralower (2022); [5]Arz *et al.* (2004); [6]Mancini *et al.* (1989); [7]Mancini (1984); [8]Arz *et al.* (2001); [9]Arenillas *et al.* (2016); [10]Arz *et al.* (2001); [11]Tantawy (2011); [12]Olsson *et al.* (1996); [13]Arz *et al.* (2022); [14]Lowery *et al.* (2018); [15]Arenillas *et al.* (2006); [16]Denne (2007); [17]Bralower *et al.* (1998); [18]Denne *et al.* (2013); [19]Keller *et al.* (2011); [20]Pessagno (1969); [21]Smith and Pessagno (1973).

Source: Paleogene planktic foraminiferal biozones after Wade *et al.* (2011); Cretaceous planktic foraminiferal biozones after Gale *et al.* (2020); Paleogene calcareous nannoplankton biozones are the NP zones of Martini (1970); Cretaceous calcareous nannoplankton biozones are the CC zones of Sissingh (1977). Age calibrations are from Gradstein *et al.* (2020).

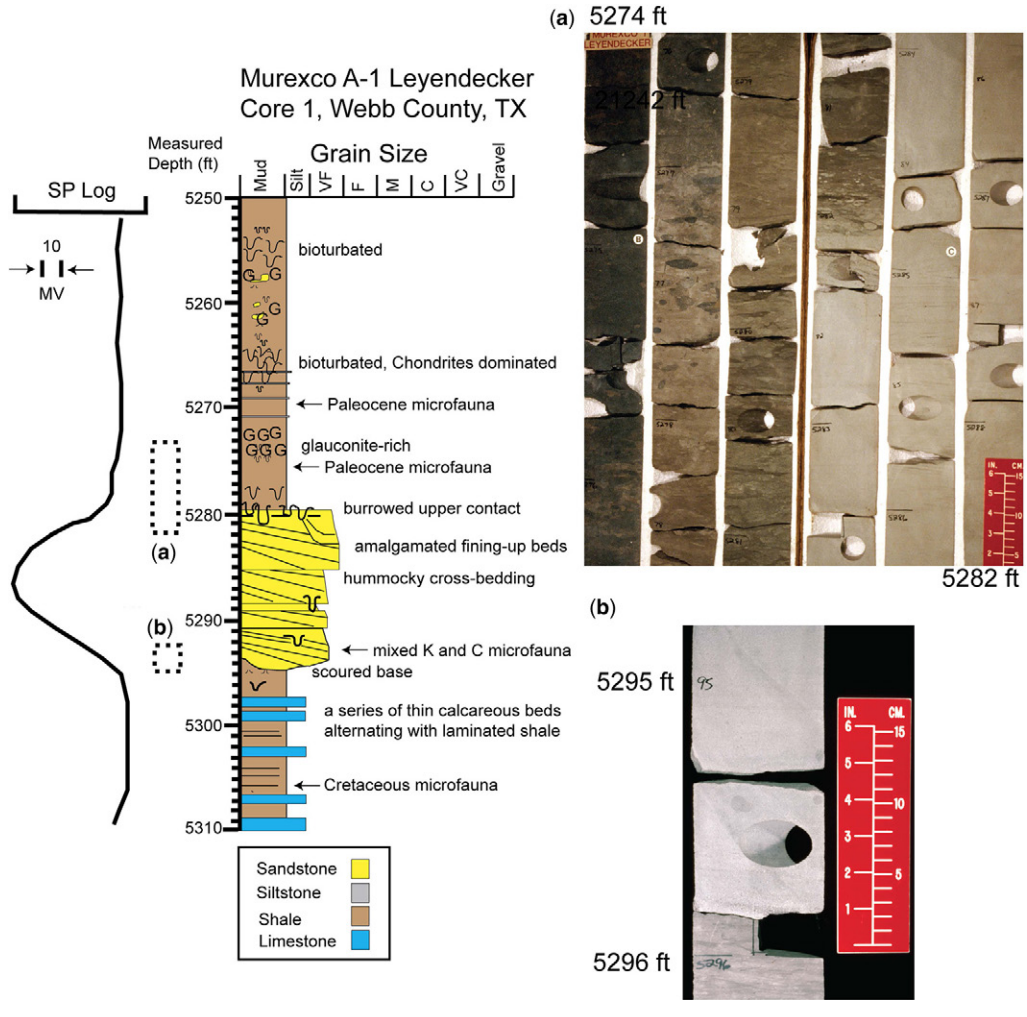

Fig. 5. Escondido Sandstone in Leyendecker #A-1 well of Webb County, Texas. Core of Upper Escondido in south Texas well; (**a**) Core photo of upper portion of core (5274–5282 ft); and (**b**) Core photo of base of sandstone showing scour. For locations see Figure 5. Source: Leyendecker #A-1 Figure from Snedden and Galloway (2019).

palaeovalleys eroded into the Delgado Sandstone Member of the Potrerillos Formation, which correlates with the upper part of the Escondido Formation (Lawton *et al.* 2005, 2020).

The upper contact of the Maastrichtian is disconformable across virtually all of the Gulf of Mexico Basin (Fig. 3). The amount of missing time varies around the basin based on proximity to the impact site, but most all surface localities and subsurface wells show an obvious erosional surface at the K–Pg boundary, evidence of current activity or disturbance associated with the impact event. An obvious erosional surface separates fossiliferous spherule-rich beds of the basal Danian deposits (often cross-bedded sandstone) from the underlying non-spherule bearing beds of Cretaceous age in the Alabama embayment (Mancini *et al.* 1989; Olsson and Liu 1993; Olsson *et al.* 1996; Hart *et al.* 2013; Witts *et al.* 2018), Texas (e.g. Smit *et al.* 1996; Bourgeois *et al.* 1988; Hart *et al.* 2012; Yancey and Liu 2013) and northeastern Mexico (e.g. Arz *et al.* 2001, 2022). At International Oil Discovery Program (IODP) Site M0077 on the peak ring of the Chicxulub Crater (location 8 of Figs 3 & 4), the pre-impact strata are absent, and impact breccia sits on top of uplifted granite of mid-crustal depth (Morgan *et al.* 2016; Xaio *et al.* 2017). The onshore Yaxcopoil-1 borehole, located in the annular trough of the crater, penetrated poorly dated Campanian–Maastrichtian age shallow water carbonates (Kring

2005). At the deepwater Cantarell Field complex in the Campeche Embayment (location 8 of Figs 3 & 4), 300 km from the centre of the Chicxulub crater, the Chac Limestone below the boundary unit breccia at the Cantarell Field complex could be as old as Turonian (Grajales-Nishimura *et al.* 2000; Aquino-Alberto 2010). To the NE of the crater, the K–Pg boundary deposit rests on sediments ranging in age from Campanian to Barremian (Bralower *et al.* 1998; 2020). Seismic (Sanford *et al.* 2016) and tsunami waves (Range *et al.* 2022) propagating from Chicxulub probably reached Gulf of Mexico locations on a time scale of a few minutes to a few hours after impact, respectively, and caused extensive mass wasting and platform margin collapse (e.g. Denne and Blanchard 2013; Denne *et al.* 2013). These extensive erosion and disturbance of the latest Maastrichtian present a challenge in reconstructing the depositional palaeogeography.

Removal of pre-impact strata by mass wasting events triggered by the Chicxulub impact is also observed elsewhere in the subsurface of the Gulf of Mexico at considerable distances from the impact site. Truncation of Maastrichtian through Oxfordian intervals is evident in deep oil and gas wells, though this varies from east to west in the northern Gulf of Mexico (Weimer *et al.* 2016). In most drilling locations of the northwestern Gulf deepwater, the K–Pg basal contact overlies some portion of the Maastrichtian and/or Campanian section. However, in the northeastern Gulf deepwater, a greater degree of 'missing time' is observed with Cenomanian and older strata absent below the K–Pg boundary (Scott *et al.* 2014).

This northeastern Gulf of Mexico area is closer to the impact site and possibly better aligned with a pre-impact structural depression (Sanford *et al.* 2016; Guzman-Hidalgo *et al.* 2021). Isolated blocks of Cretaceous strata on the abyssal plain, downslope from the Florida Platform, are likely products of the enhanced mass wasting of the margin shortly after impact (Snedden *et al.* 2014; Poag 2022). The genesis of the nearby Desoto Canyon can also be linked to these impact-related physical processes (Denne and Blanchard 2013).

The lithostratigraphic chart of the Gulf of Mexico Maastrichtian and Danian (Fig. 3) also serves to illustrate the relative proportions of sandstone, carbonates (largely limestones and chalks) and mudstones present in the basin prior to the Chicxulub impact event. Maastrichtian sandstones are mainly limited in occurrence to the Rio Grande embayment and adjacent Burgos/La Popa Basin, NE Texas/north Louisiana, SE Alabama and southern Illinois. These sandstones record mainly paralic systems (deltaic and flanking shore zones) fed by the forerunners of the Rio Grande, Red and Mississippi rivers (Potter-McIntyre *et al.* 2018; Snedden *et al.* 2022). In other areas, carbonates, chalks or shales are the dominant lithology. These will be discussed in detail in later sections.

Evaporites (halite or anhydrite) are mostly absent from the Maastrichtian of the Gulf of Mexico, which is notable given interest in the role that sulfur (contained in older Cretaceous anhydrites) may have played in the destruction of life forms following the bolide impact event (Kring 2005). However, as discussed below, we can use older Pemex well-control to define the extent of an evaporitic sabkha/lagoon system in the Yucatan target rocks, though the age of these anhydrite beds is not well constrained.

Logs and cores from a well in north Louisiana (location 13 in Figs 3 & 4) show a distinct repeated section of chalk present above the *in situ* Arkadelphia Chalk of north Louisiana, likely due to low-angle thrusting related to the bolide impact over 1000 km from Chicxulub (Fig. 6; Shellhouse 2017; Muchiri 2018; Snedden and Galloway 2019). Slumping and gravity sliding related to seismic waves arriving from the impact site is a probable cause of the observed displacement here and at other many Gulf of Mexico sites (Smit *et al.* 1994; Sanford *et al.* 2016).

Detailed descriptions of the K–Pg boundary unit impact products around the basin are abundant in the literature, and readers are directed to key papers (Smit *et al.* 1996; Arz *et al.* 2001, 2022; Lawton *et al.* 2005; Schulte *et al.* 2010; Sanford *et al.* 2016). It is worthwhile to note, however, that the basal clastic unit in many localities and subsurface wells contains transported clasts with obvious similarity to the underlying stratigraphic units, giving us partial insights to the Late Cretaceous palaeoenvironments. In Cuba, the basal Cenozoic unit of the Penalver Formation incorporates clasts clearly derived from the underlying Via Blanca Formation (location 10 in Figs 3 & 4; Tada *et al.* 2003). In Cantarell field wells (offshore Mexico, location 7 in Figs 3 & 4), the 100 m thick boundary breccia includes clasts of the underlying Maastrichtian hemipelagic limestones (Grajales-Nishimura *et al.* 2000; Murillo-Muneton *et al.* 2002). In northern Belize (location 9 in Figs 3 & 4), sedimentary clasts within the diamictites of the Albion Island resemble the underlying Maastrichtian Barton Creek Limestone (Ocampo and Pope 1994; Ocampo *et al.* 1996; Denne *et al.* 2013). The melt-bearing impact breccia from Site M0077 core at the Chicxulub peak ring (locality 8 in Figs 3 & 4) contains preserved Maastrichtian carbonate clasts with biogenic structures consistent with a nearby shallow marine realm populated by annelids, crustaceans and bivalves colonizing soft-grounds in marine well-oxygenated, nutrient rich conditions (Rodríguez-Tovar *et al.* 2022). At other reported K–Pg sites (e.g. La Ceiba, Puebla, in eastern

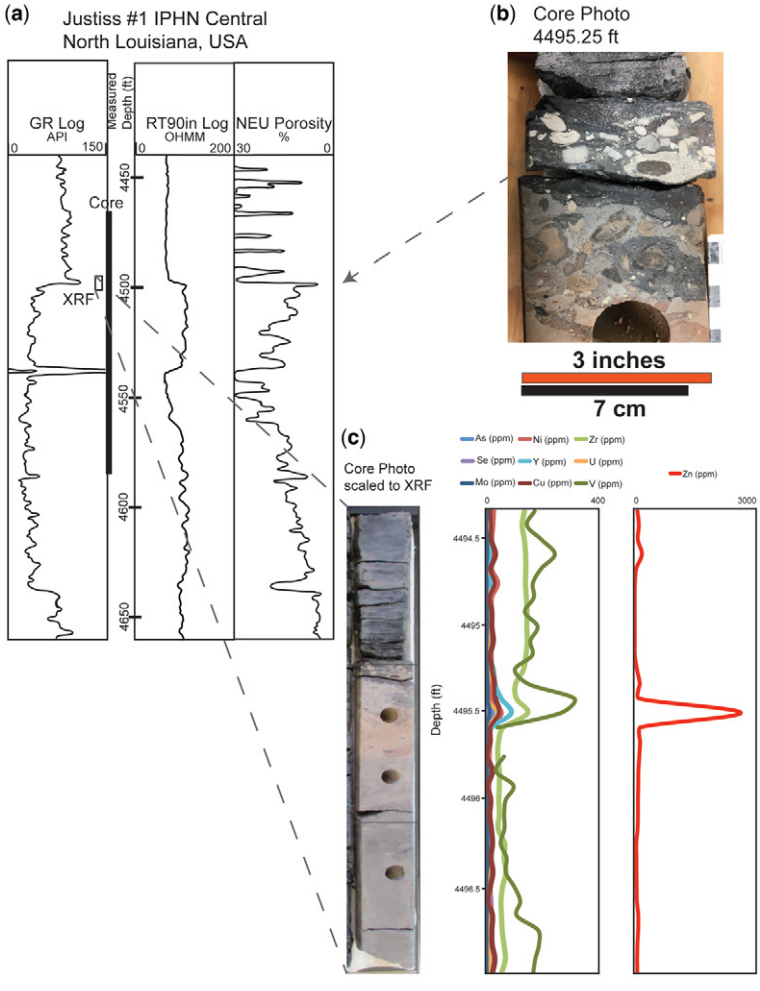

Fig. 6. Displaced and in-place chalks cored in the Justiss #1 IPHN Central well of north Louisiana. (**a**) Logs through K–Pg boundary. (**b**) Core photo from Midway–K–Pg boundary, 4495.25 ft measured depth. (**c**) Expanded core photo and X-ray fluorescence results including zinc proxy for iridium. For location see Figure 5. Abbreviations: GR, gamma ray; API, American Petroleum Institute units; XRF, X-ray fluorescence. Source: (c) from Snedden and Galloway (2019).

Mexico), the K–Pg boundary unit consists of the deposit of a single turbidity current interbedded in a thick marly shale interval deposited at bathyal depths greater than 1000 m (Arz *et al.* 2001, 2022).

As mentioned above, post-impact Upper Escondido sandstones yielded 66 Ma zircons with a provenance signature of the palaeo-Rio Grande River, suggesting derivation from local Cretaceous paralic systems (location 2 in Figs 3 & 4; Snedden *et al.* 2022). Thin, locally sourced event bed sandstones are common in other Gulf of Mexico K–Pg outcrops, likely due to offshore transport by a variety of impact-related processes, including tsunami waves or backwash-return flows, and/or offshore-directed sediment gravity flows (e.g. Lawton *et al.* 2005; Hart *et al.* 2012, 2013; Schulte *et al.* 2012; Yancey and Liu 2013; Leighton *et al.* 2017). Numerical models of tsunami propagation in the first minutes after the Chicxulub impact point to seafloor scour and sediment transport up to 10 000 km from the impact origin (Range *et al.* 2022).

Thus, we can infer much about the Maastrichtian (and underlying units) from observations of the K–Pg breccia and sandstone units that are common components of the K–Pg boundary unit. This, in turn, is factored into our depositional reconstructions of the latest Maastrichtian sea- and landscape.

Maastrichtian global eustasy v. regional relative sea level

Estimates for global and local sea level during the Maastrichtian and Danian stages vary significantly in terms of magnitude but are remarkably similar in terms of temporal trends (Fig. 7). Original estimates of global sea level changes on the order of 100 m ± (Hardenbol *et al.* 1998; Haq and Shutter 2008) have since been modified as much as 50% less, reflecting improvements stemming from back stripping and other techniques to delineate the effects of subsidence, loading and compaction in assessing global sea level changes (Miller *et al.* 2020). Current consensus is that during most of the Phanerozoic, global eustatic change has been less than ±100 m from the present-day level (Snedden and Liu 2011).

The Gulf of Mexico generally reflects the ice-free hothouse/greenhouse world of the Late Cretaceous to Eocene. After reaching a secondary peak in rising sea levels at the Santonian–Campanian boundary, global sea levels trend moderately lower, a pattern that reverses in the late Danian (Fig. 7). This is consistent with various reconstructions of global trends in palaeoshoreline migration and continental land mass inundation history (synthesized in Heine *et al.* 2015).

Another important reflection of sea level trends in the Late Cretaceous of the Gulf of Mexico Basin is the presence and widespread distribution of chalks. Chalks form by the massive accumulation of coccolith plates covering the surface of single-celled marine phytoplankton. Chalks are common in deep sea palaeoenvironments, though shelfal chalks are known (e.g. Bottjer 1981). Chalk deposits are found in the Upper Cretaceous strata of Europe (e.g. maps of M. J. d'Omalius d'Halloy) and in the WIS and Gulf of Mexico (Bottjer 1986; Snedden and Galloway 2019).

The Niobara Formation (Coniacian to Campanian) of the WIS is a chalk-bearing interval that represents the final major marine transgression of the seaway (Hancock and Kaufman 1979; Drake and Hawkins 2021). Continued high sea level and a direct connection between the WIS and Gulf of Mexico are signaled by successive accumulations of chalks in the Austin Group, Pecan Gap and Annona until the latest Campanian (Bottjer 1986). Chalk deposition persisted into the early Maastrichtian but showed signs of shallowing locally into

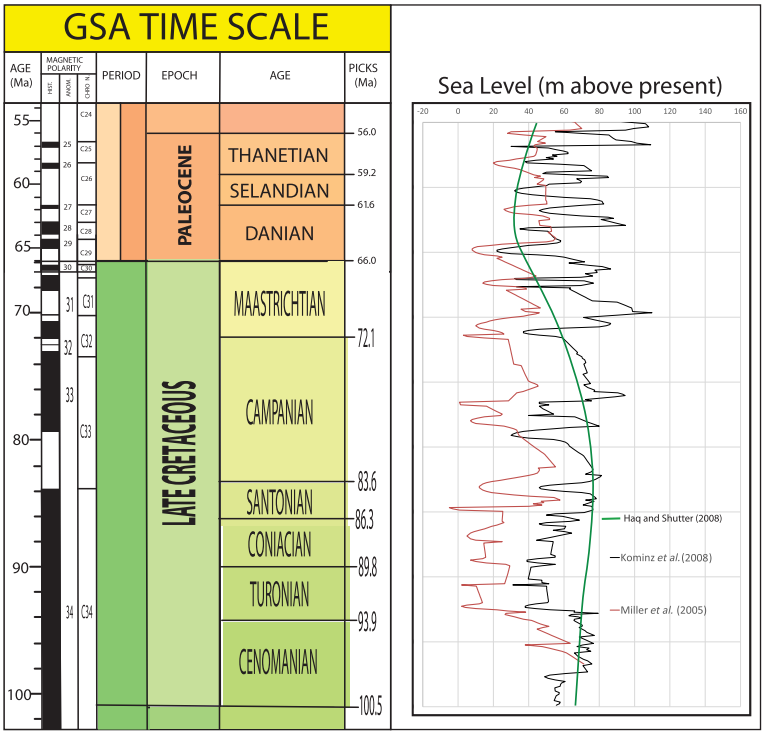

Fig. 7. Maastrichtian to Danian sea level trends. Source: sea level curves compiled in Miller *et al.* (2020), including Miller *et al.* (2005), Kominz *et al.* (2008) and Haq and Shutter (2008). Timescale from Geological Society of America (2022).

middle shelf water depths (15–50 m), as estimated from the Saratoga Chalk in SW Arkansas (Bottjer 1981). Formation of numerous discontinuity surfaces in these chalks indicates vigorous current action associated with progressive closure of the connection with the WIS. Withdrawal of the sea to the north can be linked to the earliest stages of the Laramide orogeny and a progressively falling global sea level. This restricted chalk deposition to the flooded Mississippi embayment (Arkadelphia Formation) in the late Maastrichtian, but by this point, the marine connection between the Gulf of Mexico and WIS had been severed.

Tectonic/plate reconstructions of the northern and southern Gulf of Mexico

The Maastrichtian Stage was a time of active tectonics, both surrounding and within the greater Gulf of Mexico Basin. In the WIS of the USA, thin-skinned deformation related to the Sevier orogeny began in the Late Jurassic and continued into the Paleogene, overlapping temporally but not spatially with Laramide thick-skinned tectonics (Weil and Yonkee 2012). The Mexican Orogen is a similar series of episodic shortening events that include the Maastrichtian and earliest Danian Stage (Fitz-Díaz *et al.* 2018). Synorogenic turbidites began to accumulate on top of relict shallow water platform carbonates in the Tampico–Misantla basin in the Maastrichtian, and these were in turn folded beginning in the early Cenozoic (Fitz-Díaz *et al.* 2014). A folded unconformity separates highly deformed Cretaceous strata from mildly deformed Paleogene strata. However, areas closer to the Chicxulub impact site in Yucatan (e.g. Sureste Salt basin) were relatively unaffected, with salt tectonics playing a larger role (Rowan *et al.* 2022).

The same can be said for the northern Gulf of Mexico, where the far field influence of the Laramide orogeny was mainly manifested in increased sediment load in the palaeo-Rio Grande system, which deposited the Maastrichtian San Miguel, Olmos and lower Escondido sandstones (Snedden and Kersey 1982; Tyler and Ambrose 1986). Other nascent rivers contributed sediment to the Nacatoch Sandstone of north Texas (palaeo-Red River), eastern Louisiana and shore zones of the Owl Creek–Providence–Ripley sandstones further east (palaeo-Mississippi; Snedden and Galloway 2019; Snedden *et al.* 2022).

Laramide crustal shortening continued past the Danian Stage, with sediment-distribution networks filling in intermontane basins and eventually forming large trunk rivers flowing SE toward the Gulf of Mexico (Galloway *et al.* 2011; Snedden *et al.* 2018*a*). In Mexico, uplifts and adjacent foreland troughs were generated, reactivating basement structures and creating a general basinward tilt (Alzaga-Ruiz *et al.* 2009).

The large-scale driver for this Late Cretaceous to Eocene deformation is thought to be subduction of the Farallon slab (Fitz-Díaz *et al.* 2018). A restoration at Maastrichtian (70 Ma) time shows the position of the Chortis block, an important element defining the Gulf of Mexico–Caribbean basin boundary (Fig. 8; Pindell *et al.* 2023). The Greater Antillean arc, which included the restored Cuban block, collided with the southern edge of North American continental lithosphere, which included the Yucatan block, to form the high-grade Chuacús complex of central Guatemala (Martens *et al.* 2012). This collision formed the southern boundary of the Gulf of Mexico Basin, which, at the time, consisted of a deepwater foreland basin to the north where the Sepur–Chemal flysch deposits accumulated (Fig. 3; Pindell *et al.* 1988; Pindell and Barrett 1990; Lawton *et al.* 2020; Martens and Sierra-Rojas 2021). The Colon fold belt of Honduras was probably co-linear with the Chuacús complex in the late Maastrichtian but was subsequently offset by Cenozoic rotation and translation (Rogers *et al.* 2007; Pindell *et al.* 2011).

In most global palaeogeographical reconstructions, these structures and tectonic boundaries are just north of the Central American Seaway connecting the Pacific and Atlantic oceans (Fig. 1; Scotese and Dreher 2012; Scotese 2021). This is confirmed by macrofossil radiation patterns controlled by interpreted surface current circulation. Larvae of rudist bivalves dispersed with these surface currents appear to have migrated initially westward and then NW into the northern Gulf of Mexico Basin (Johnson 1999). Proximity of the Cuban arc to Yucatan in the Late Cretaceous may have facilitated these migrations by providing a western topographic barrier adjacent to the Gulf of Mexico. This, in turn, requires shallow water depths as preferred by rudists on both platforms, which informs our depositional palaeogeographical reconstruction discussed in later sections. Maastrichtian decapods native to the Mississippi embayment are also found in the WIS (Kornecki *et al.* 2017). Emplacement of the Panama–Costa Rica arc in the Cenozoic later closed the Central American Seaway between North and South America (Montes *et al.* 2015; O'Dea *et al.* 2016).

The structural configuration at the Top Cretaceous horizon is largely a function of crustal types, long-lived basement highs and lows, post-Cretaceous sediment deposition and loading and the Chicxulub impact crater (Fig. 9). The Gulf of Mexico Basin is mostly underlain by deep crust that transitions from basin centre oceanic crust to continental crust on the basin margins. A marked deepening of the Top Cretaceous is coincident with

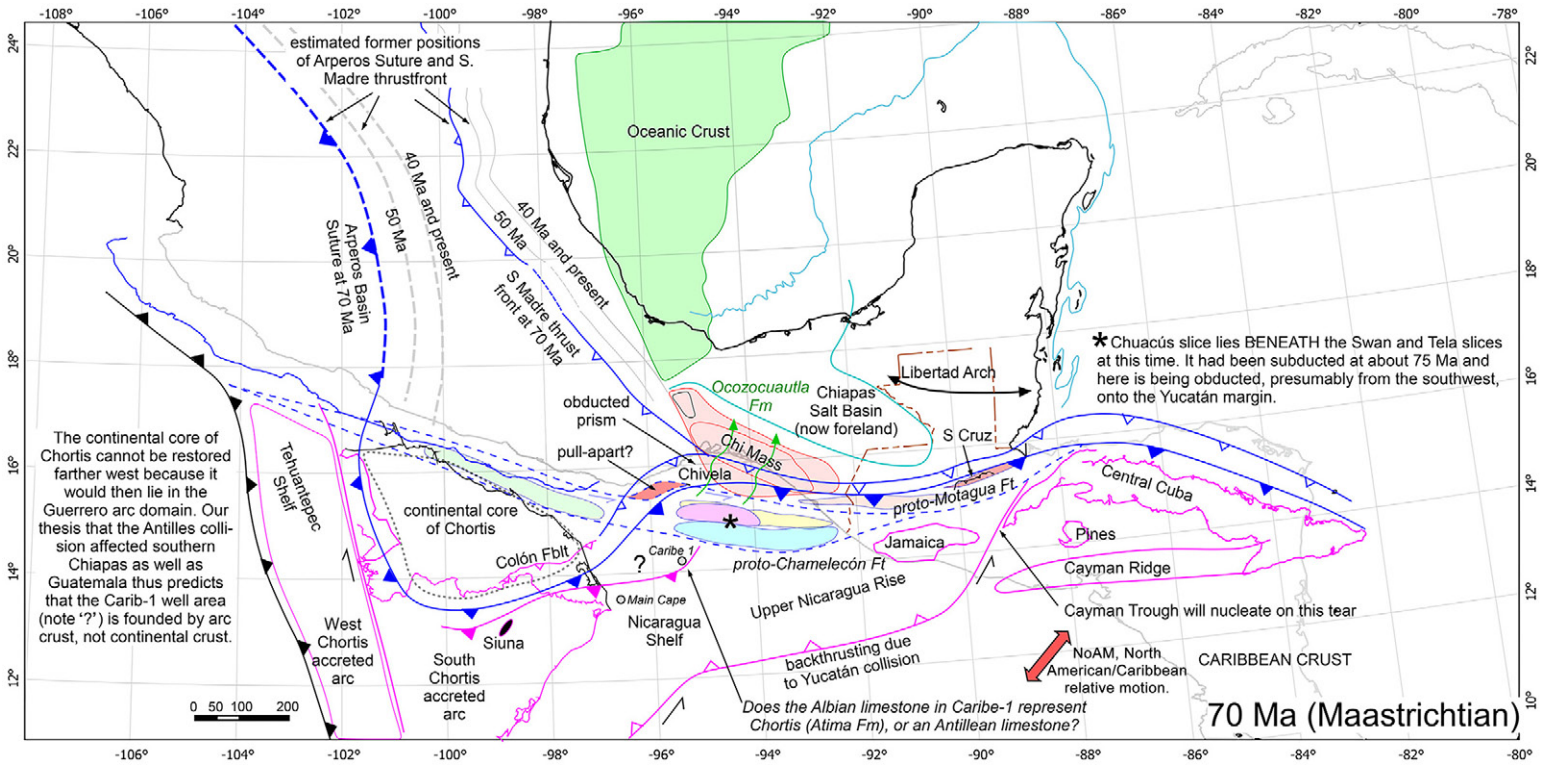

Fig. 8. Maastrichtian (70 Ma) restoration of southern Mexico–Caribbean region. Source: from Pindell *et al.* (2023).

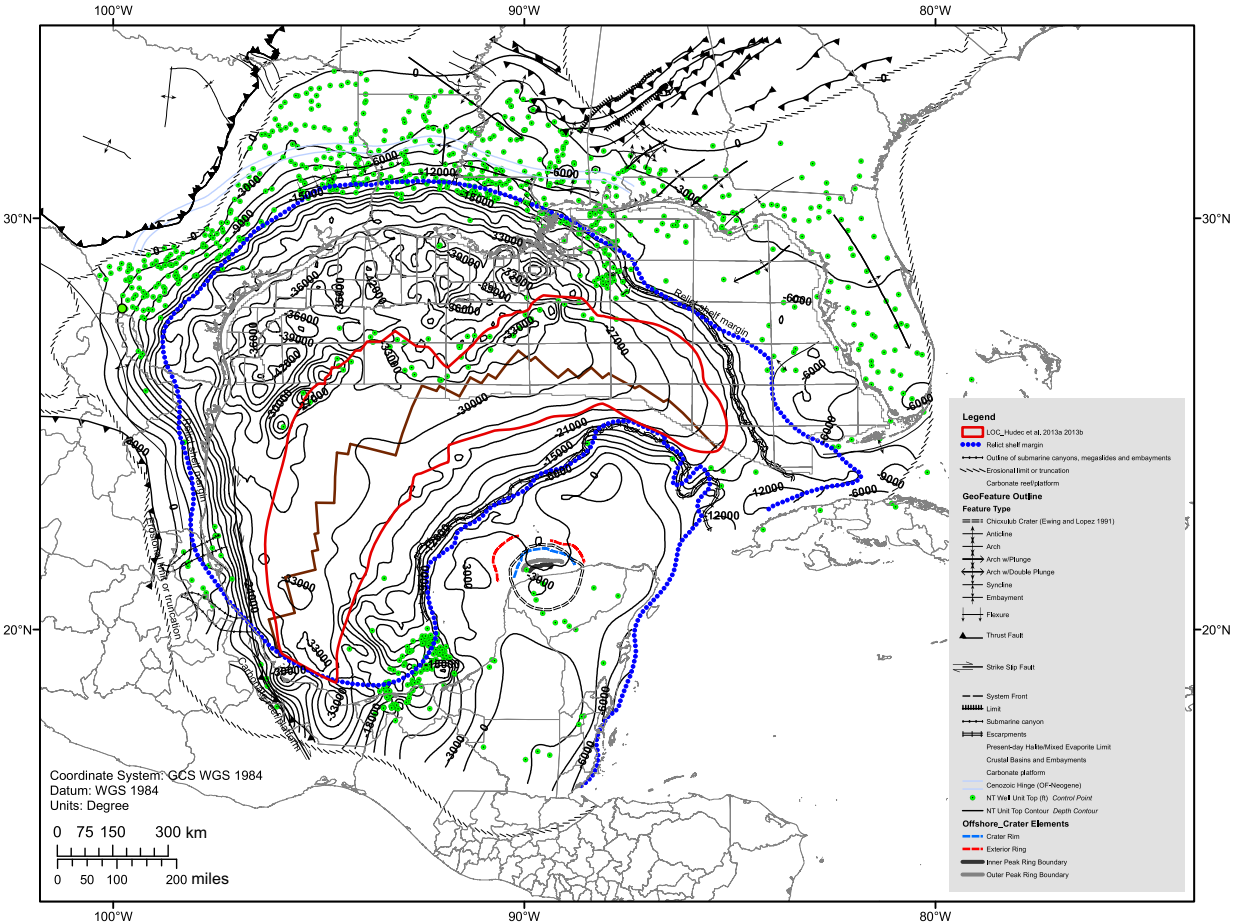

Fig. 9. Top Cretaceous structure map (CI = 3000 ft; 914 m) showing underlying deep crustal types and well control (green-filled circles). Abbreviations: WGS, World Geodetic System; GCS, geographic coordination system. Source: important structural trends including Chicxulub crater derived from Ewing and Lopez (1991); offshore crater features from Gulick *et al.* (2013); limit of ocean crust (LOC; red line) from Hudec *et al.* (2013); dotted blue line is relict Cretaceous shelf margin from Snedden and Galloway (2019).

the relict basin-rimming shelf margin, where photic zone carbonates were limited by large increases in palaeowater depth due to subsidence over thinner transitional continental crust (Snedden and Galloway 2019). Local structural highs and lows trending normal to this basin rim can be related to reactivated basement blocks and areas of post-Cretaceous sediment loading. The Chicxulub Crater overlaps with a NW–SE trending pre-impact basin called the north Yucatan trough, which played a role in shaping post-impact progradational fill of the crater (Guzman-Hidalgo *et al.* 2021).

Maastrichtian palaeoclimate

The well-documented generally ice-free conditions of the Cretaceous (e.g. Scotese *et al.* 2021) continue to be of great scientific interest with enhanced need for climate change modelling. There is also impetus for understanding how the extant surface winds distributed the Chicxulub impact products, including ejecta and potential sulfur aerosols (Kring 2007).

High palaeotemperatures in the Maastrichtian are also known from palynological studies showing expansion of high latitude forests that likely inhibited development of sea ice and glaciers (Upchurch *et al.* 1999). The proposed surface flow kinematics of Johnson (1999) mentioned earlier thus also explains a progressively warming Cretaceous world and low gradients of temperature equator to pole.

A late Maastrichtian global warming associated with onset of massive Deccan Trap volcanism may have occurred within the final 400 kyr before the end of the Cretaceous (Gilabert *et al.* 2021). However, consensus is that related greenhouse gas emissions were far too weak to cause the terminal Cretaceous global mass extinctions (Hull *et al.* 2020).

Within the northern Gulf of Mexico Basin, palaeoclimate indicators indicate temperate, humid conditions. Palynology from the coal-bearing Olmos Formation of south Texas reveals a transition from tropical to subtropical climates (Mahmoud 2004). Maastrichtian to Paleogene age coal beds are also present in the Difunta Group of the Burgos and Sabinas Basins of Mexico (Eguiluz de Antuñano 2001; Lawton *et al.* 2021 and references therein).

Warmer and more arid conditions may have existed in the latter stages of the Cretaceous in the southern Gulf of Mexico, though these evaporites are poorly dated. A crude palaeogeographical map of Yucatan constructed by Lopez-Ramos (1975) depicts an Upper Cretaceous evaporitic platform, based upon the occurrence of anhydrite in several Yucatan wells, including Yucatan-1. However, later correlations suggest that the evaporitic intervals are older, likely Coniacian to Albian (Ward *et al.* 1995). Cenomanian to Albian anhydrites are particularly thick in Yucatan wells such as Ticul-1, Yucatan-1, -2, -4 and -5 (Lopez-Ramos 1975). Some uncertainty about the pre-impact Maastrichtian lithology within 50 km of the impact centre exists because this section was removed by the bolide impact.

The well nearest the impact centre with possible preserved Maastrichtian strata is the International Continental Scientific Drilling Programme (ICDP)-Yaxcopoil-1 core well, drilled in the annular trough, about 60–65 km from the crater centre. Importantly, it was positioned 15 km outside of the crater excavation cavity (location 14 in Fig. 4; Kring 2005). Below the impact-related breccia and suevite dykes is a 500 m thick shallow water carbonate that lacks age diagnostic fossils and is interpreted to range in age from Campanian–Maastrichtian (Arz *et al.* 2004) to Turonian (Stinnesbeck *et al.* 2004). Anhydrite is present in layers and as nodules, with the thickest anhydrite beds (2 to 11 m) found in the 160 m total cored thickness of unit D of Stinnesbeck *et al.* (2004). In other units, anhydrite is absent or present as rare thin beds. Unit D, which could be older than Maastrichtian, is interpreted as formed in a restricted interior platform or sabkha with intertidal to supratidal evaporitic deposition. In other units where evaporites are thin or absent, subtidal limestones and dolomites are dominant (Stinnesbeck *et al.* 2004).

A similar pattern is observed in cuttings-based lithologic reports from the Pemex well Colon-1, located about 280 km from the crater centre (well location 16 in Fig. 4). The well penetrated a 500 m aggregate succession of anhydrite, limestone and dolostones between the Top Cretaceous (Cretaceous Superior as used locally in Mexico) and Turonian (Eagle Ford equivalent). A considerably thicker (>2000 m) Albian and older succession of anhydrite was penetrated lower in the same borehole.

The Quintana Roo-1 well was drilled in east-central Yucatan (well location 15 in Fig. 4), targeting Lower Cretaceous carbonate objectives over a gravity anomaly. The well encountered numerous anhydrite beds below the Top Cretaceous, though there was limited biostratigraphic information and the assignment of a Maastrichtian age to the anhydrites is tenuous.

Observations from Pemex wells Colon-1 and Quintana Roo-1, as well as the continuously cored ICDP borehole Yaxcopoil-1, point to a platform-centred evaporitic sabkha present in central Yucatan beginning in the Early Cretaceous, which progressively contracted in size through the Turonian to Maastrichtian stages. There is, however, some uncertainty surrounding the Maastrichtian ages of samples of the three wells, so it is possible that conditions suitable for evaporite formation may not have continued into the Maastrichtian on the Yucatan

Platform. Therefore, a logical deduction from the subsurface occurrence of anhydrite in these wells is that at the impact target zone, strata deeper and older than the Maastrichtian are probably required to generate large volumes of sulfur sourced by *in situ* anhydrite beds necessary for the generation of sulfur-rich aerosols and runoff terminating land and sea fauna and flora at the end of the Cretaceous (Kring 2005, 2007).

Depositional palaeogeography of the Gulf of Mexico Basin

Our reconstruction of the Maastrichtian depositional palaeogeography reflects underlying Gulf of Mexico Basin structure, plate tectonics, chrono- and lithostratigraphy, sea level and palaeoclimate history (Fig. 10). Our discussion moves from the basin margin where palaeorivers rout siliciclastics from source terranes to the abyssal plain where deep water carbonates and chalks accumulated. As will be discussed in a final section, this pre-impact land- and seascape influenced the type and distribution of impact products and related physical transport processes.

Palaeoriver to shoreline siliciclastics

Two significant palaeorivers distributed sediment to the Gulf of Mexico Basin in the Maastrichtian (Fig. 10; Snedden *et al.* 2022). These palaeorivers are recognized from the presence of subsurface depocentres, areas of substantial accumulation of sandstones, typically greater than 152 m (500 ft; Galloway *et al.* 2011). The depocentres represent time-averaged depositional trends, reflecting long-term sediment supply modulated by subsidence and eustatic accommodation trends. Examination of wells penetrating these large depocentres shows often log motifs or patterns that are characteristic

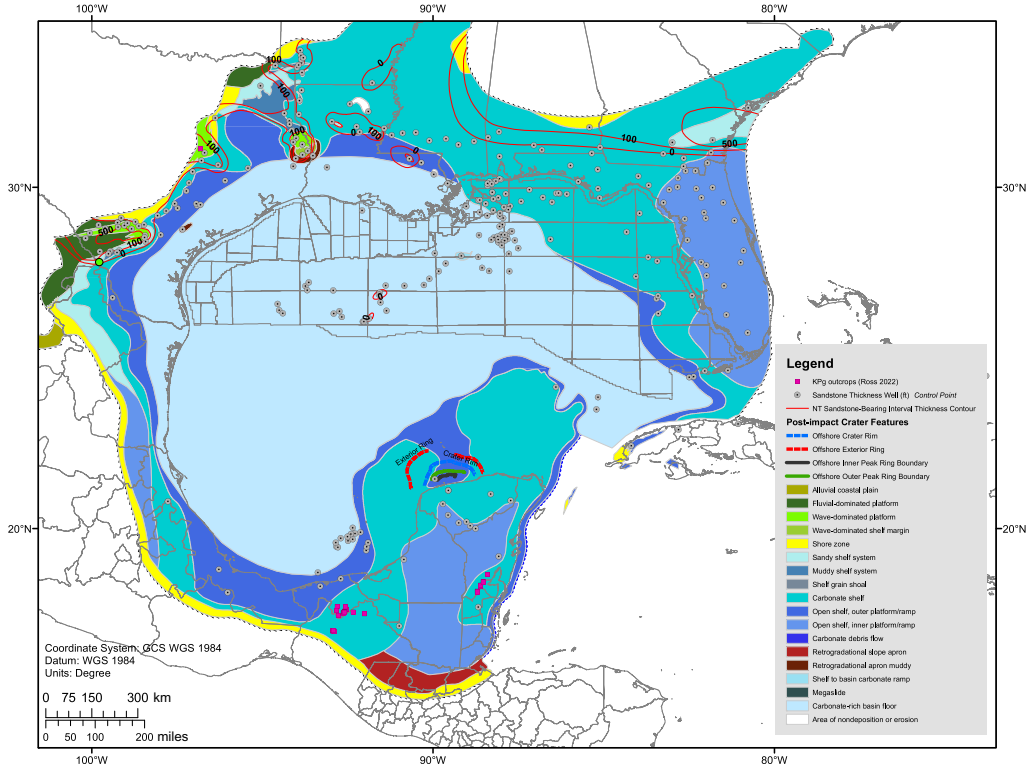

Fig. 10. Maastrichtian depositional palaeogeography with unit specific well control (grey-filled dotted circles). Dotted blue line is relict Cretaceous shelf margin from Snedden and Galloway (2019). Superimposed contours are sandstone-bearing interval thicknesses (variable contour interval from 0 to 1000 ft; 0 to 300 m) from well control. Hachured line shows erosional limit due to Cenozoic uplift and truncation associated with Appalachian rejuvenation (USA) and Chiapanecan orogeny (Mexico). Source: dotted blue line is relict Cretaceous shelf margin from Snedden and Galloway (2019).

of fluvial-dominated delta systems (Snedden and Galloway 2019).

Maastrichtian sandstones are present in the Burgos Basin of south Texas and Mexico. Sandstones found within the Escondido, Olmos and San Miguel Formations (Snedden and Kersey 1982; Snedden and Jumper 1990; Snedden 1991) are rough age equivalents of the lower part of the Difunta Group (location 3 in Figs 3 & 4; Lawton *et al.* 2009). Samples from the upper portion of the Escondido in a south Texas well described earlier (location 2 in Fig. 4) contain a detrital zircon U–Pb age subset dominated by Cenomanian and Jurassic age peaks, which signal that sediment routing into the Rio Grande embayment was likely coming from SE Arizona and NE Mexico (Snedden *et al.* 2022). However, absence of an Early Cretaceous western Mexico arc detrital zircon U–Pb age subset, which is present in the age-equivalent Delgado Sandstone Member of the La Popa Basin (Lawton *et al.* 2009, 2021), implies that much of the evolving palaeo-Rio Grande drainage flowed north of the Burro–Tamaulipas arch towards this south Texas depocentre.

The Olmos delta is the largest siliciclastic system of the palaeo-Rio Grande, as depicted in the depositional palaeogeography (Fig. 10). In subsurface wells, it includes mixed fluvial and wave-influenced depositional facies called the 'updip Olmos', and further basinward, a shelfal sandstone interval called the 'downdip' Olmos (Snedden and Kersey 1982; Snedden and Jumper 1990; Waltrip 2020). High eustatic sea levels in the Maastrichtian promoted development of wide marine shelves and deposition of extensive sheet-like neritic sandstone bodies here.

The younger Escondido Sandstone is exposed along the Rio Grande but also occurs in the subsurface (Snedden 1991). The K–Pg boundary at the outcrop just updip of location 2 in Fig. 4 is a hardground (Cooper 1973), like that observed at the K–Pg boundary in other localities (Smit *et al.* 1994). However, in the Tom Walsh–Owen Field complex located nearby, a series of thin (5–10 m scale) sand sheets in the Upper Escondido are potential products of impact-related tsunami backwash, with a scoured base and hummocky cross-bedding (Fig. 5; Kinsland and Snedden 2016). The San Miguel sandstones, by contrast, form large sand ridge-like features thought to represent transgressed deltas and shore zones (Weise 1980; Mahmoud 2004; Trevino *et al.* 2007).

South of the US–Mexico border, outcrops of the Difunta Group (location 3 in Figs 3 & 4) include the Delgado Sandstone Member of the Potrerillos Formation, a roughly 20 m (65 ft) thick sandstone succession extending across the K–Pg boundary (Lawton *et al.* 2001, 2005, 2009, 2021). The lateral extent of the Delgado outside of the La Popa, Sabinas and Burgos Basins is less well-documented because of later Laramide–Hidalgoan tectonics. For our reconstruction, we assume the pre-impact existence of a narrow Maastrichtian shore zone extending along the entire Mexican Cordilleran front to the plate boundary in the Chuacús complex. Exposures all along this trend (Los Ramones, Rancho Nuevo, Sierrita–Las Rusias, Penon, Porvenir, Mulato–Bruselas, La Lajilla, Mesa de Llera, Mimbral, La Ceiba and Bochil) in eastern Mexico show the presence of post-impact sandstones (Smit *et al.* 1994), thus arguing for a laterally continuous sand source, such as a wave-dominated shore zone.

We place the erosional truncation line just updip of this shore zone, assuming Laramide exhumation of most of the linked coastal plain and any small fluvial systems. Some of these coastal plain streams were possible forerunners of Paleocene–Eocene systems that are documented as flowing into Chicontepec and Bejuco canyons (Lawton *et al.* 2009; Snedden *et al.* 2018*b*). Scattered outcrops west of this erosional limit do exist but these are all plutonic or volcanic components of the Late Cretaceous arc (Fitz-Díaz *et al.* 2018).

The presence of a second important palaeoriver in the northern Gulf of Mexico is based on the presence of Maastrichtian deltaic sandstones in north Texas and Louisiana called the Nacatoch Formation (location 13 in Figs 3 & 4; McGowen and Lopez 1983; Kennedy 2013). We infer that this palaeo-Red River drained mid-Appalachian, Ouachita, Grenville, Mid-Continent and Wyoming–Superior source terranes. However, no detailed detrital zircon analyses of the Nacatoch have been published, but we assume similar provenance to the underlying Cenomanian–Turonian Woodbine Sandstone deposited by the palaeo-Red River (Blum and Pecha 2014).

Smaller palaeorivers flanked by wave-dominated shore zones are inferred from outcrops in the eastern margin of the Mississippi embayment, including exposures of Maastrichtian age sandstones with local lithostratigraphic names of Owl Creek–Nixon (Witts *et al.* 2018), Providence (Salvador 1991) and Ripley (location 12 in Figs 3 & 4; Jackson *et al.* 2021). Deposition of the Owl Creek Sandstone extends across the K–Pg boundary including spherules and sediments clearly derived from underlying Maastrichtian strata (Witts *et al.* 2018). The sandstones at the outcrop and in downdip wells are relatively thin or absent, suggesting possible along shore dispersal from a forerunner of the palaeo-Mississippi River, which is thought to have deposited the underlying Ripley Formation (Jackson *et al.* 2021).

Shelf to deep marine carbonates

Siliciclastic systems, however, cover a relatively small portion of the Maastrichtian (pre-Chicxulub impact) map area. Shallow to deep marine carbonate palaeoenvironments occupy a much greater

percentage of Gulf of Mexico seascape (Fig. 11). The carbonate-dominated realm ranging from carbonate grainstones of the shore zone and inner shelf to basin floor carbonate mudstones is illustrated in this depositional palaeogeography, based on well control and outcrops in the USA and Mexico. Shallow water and shelf margin reefs were prominent by the Early Cretaceous in both Mexico and the USA. Platform margin systems continued in the northern Gulf of Mexico Basin until diminishing in the Albian, reflecting progressive sea level rise and oceanic anoxic events (Phelps *et al.* 2014, 2015). Isolated carbonate platforms in Mexico persisted into the Cenomanian. The Yucatan Platform margin may have developed local reef buildups later removed by K–Pg impact failure processes (Sanford *et al.* 2016). Prominent headscarps and mass transport complexes are noted along large portions of the present-day Yucatan margin (Hübscher *et al.* 2023).

The presence of a pre-impact structural syncline extending across the northern Yucatan Platform was first identified on 2D seismic sections by Sanford *et al.* (2016), and later mapped in detail by Guzman-Hidalgo *et al.* (2021), who named it the Yucatan Trough. Our palaeogeography includes the northern Yucatan Trough in the latest Cretaceous palaeogeography (Fig. 11), where outer shelf carbonate depositional systems intrude upon the shallower shelf deposits of the rest of the Yucatan Platform. There is some uncertainty regarding the southern arm of the Yucatan Trough given the impact-related stratal removal and limited biostratigraphic resolution in older Yucatan wells drilled by Pemex (Ward *et al.* 1995). Thus, we have not included this southern portion of the Yucatan Trough in the pre-impact palaeogeographical map.

Our depositional reconstruction also assumes that the relict shelf margin of the northern Gulf, largely

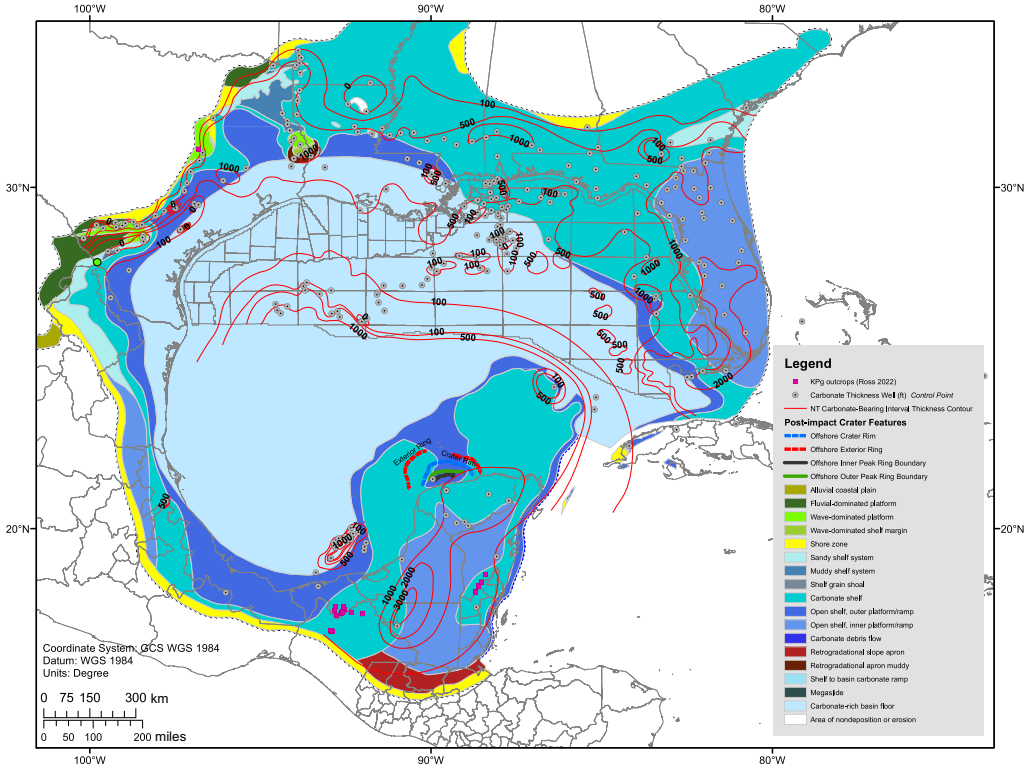

Fig. 11. Maastrichtian depositional palaeogeography with well control (dotted grey-filled circles). Dotted blue line is relict. Superimposed contours are carbonate-bearing interval thicknesses (variable contour from 0 to 1000 ft; 0 to 300 m) from well control. Hachured line shows erosional limit due to Cenozoic uplift and truncation associated with Appalachian rejuvenation (USA) and Chiapanecan orogeny (Mexico). Legend shows interpreted palaeoenvironments (this paper) and rock types in Late Cretaceous arc from Sickmann and Snedden (2021). NT, Navarro–Taylor supersequence. Source: Relict shelf margin interpreted as updip limit of carbonate-rich basin floor. Snedden and Galloway (2019); interpreted palaeoenvironments (this paper) and rock types in Late Cretaceous arc shown in legend are from Sickmann and Snedden (2021).

inherited from this basin-rimming system in the Early Cretaceous, marks a large increase in slope gradient and palaeobathymetry around the Gulf of Mexico Basin. Another indication of the importance of this relict shelf margin is apparent in the gross Maastrichtian–Campanian interval isochore map (Fig. 12). Thicknesses of the Maastrichtian and Campanian interval section increase significantly downdip of this margin, particularly in the northern Gulf of Mexico, where a four- to six-fold increase is documented from 2D seismic and well data.

While the gross-interval isochore map is largely restricted to the pre-Chicxulub impact strata, it is possible that in areas where the K–Pg boundary is less well-defined, some post-impact sediments are included on this map. However, observations of seismic stratal truncation, and logs showing the K–Pg unit with an upward 'fining' log motif and a sharp basal contact (e.g. Fig. 13; Scott *et al.* 2014), help differentiate the two units. In some areas (e.g. location 13 in Figs 3 & 4), the post-impact interval includes a repeated section of a portion of the underlying Cretaceous chalk (Fig. 6). Differences between the two units can be subtle locally, suggesting limited remobilization. Thus, the pre-impact lithology and thickness trends do inform us about depositional conditions and accommodation prior to the Chicxulub impact.

The depositional palaeogeography shown here mirrors these basin-scale trends. Updip of this margin, a seaward-dipping ramp from carbonate inner shelf to outer shelf varies in width depending on the local sea floor gradient (Fig. 11). The shelf is particularly narrow in Mexico. South of the northern Gulf shelf margin, an expansive basin floor or abyssal plain of mainly pelagic carbonates includes deep marine chalks, reflecting the generally global and regional high sea level state. It should be noted that

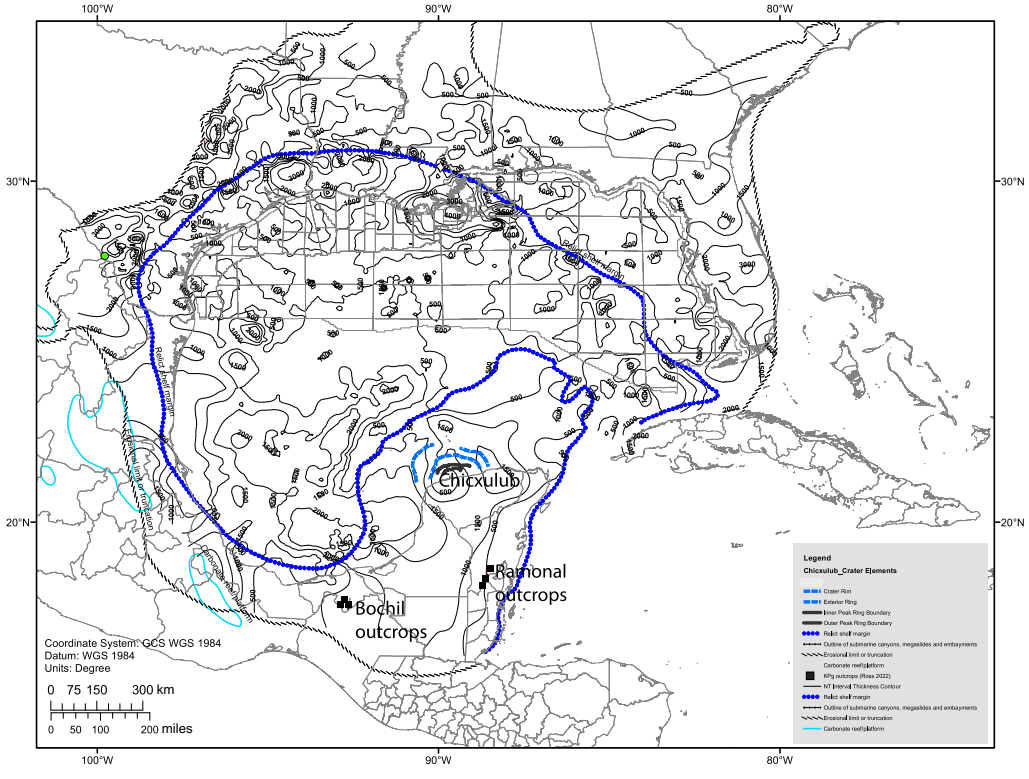

Fig. 12. Maastrichtian–Campanian gross interval thickness based on seismic and well control (see database Fig. 2). Dotted blue line is relict Cretaceous shelf margin from Snedden and Galloway (2019). Hachured line shows erosional limit due to Cenozoic uplift and truncation associated with Appalachian rejuvenation (USA) and Chiapanecan orogeny (Mexico). Important carbonate platform margin trends in Mexico (light blue lines) largely buried by the Maastrichtian Stage are derived from Ewing and Lopez (1991). Key outcrops of Maastrichtian and K–Pg in Mexico (Bochil and Ramonal) are shown by black-filled squares. Source: dotted blue line is relict Cretaceous shelf margin from Snedden and Galloway (2019); important carbonate platform margin trends in Mexico (light blue lines) largely buried by the Maastrichtian Stage are derived from Ewing and Lopez (1991).

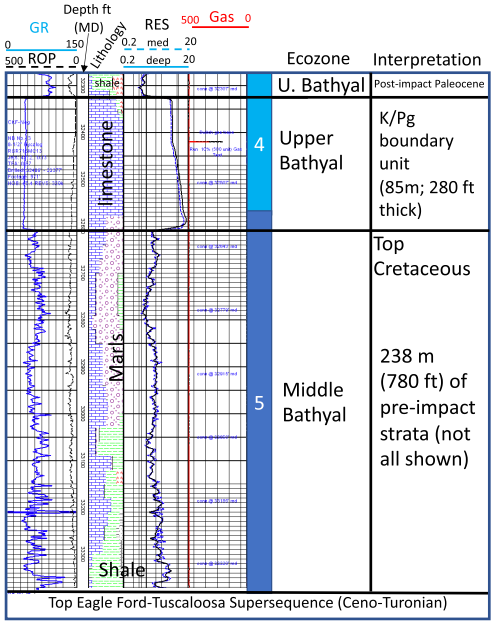

Fig. 13. Tiber well (KC 102 #1) logs and lithology from cuttings description. Abbreviations: GR, gamma ray; ROP, rate of bit penetration; MD, measured depth; RES, resistivity. Source: ecozone designations from Bureau of Ocean Energy Management reports; ecozone classification from Tipsword *et al.* (1966).

shallow water chalks are also known from areas updip of the margin (Bottjer 1986).

Calcareous mudstones and marls are also present in the basin, generally where dilute turbidity flows carried fines from deltaic systems into the deep basin. In the deep basin, however, there are a limited number of wells that provide lithology, age and palaeobathymetric information. Palaeobathymetry remains an important question and is discussed below in the section describing map uncertainties.

Deep marine shales of the Sepur–Chemal formations accumulated in a developing foreland basin north of the Chuacús mega-shear boundary (Lawton *et al.* 2020). High rates of subsidence in this narrow zone in Guatemala yielded palaeowater depths far greater than those of the coeval Mendez of the Poza Rica–Tuxpan platform area (location 4 in Figs 3 & 4; Lawton *et al.* 2020). A short transition from this deep marine to a broad sabkha/lagoon where evaporites formed would be expected but not unusual for a foreland basin like this. Another foreland basin area where palaeowater depths may have locally reached bathyal depths (>1000 m) is in the Veracruz Basin near Puebla, Mexico (Arz *et al.* 2001).

The Maastrichtian section in Cuba is an aggregate of marine platform carbonates, exposed land masses and deep marine shales (location 10 in Figs 3 & 4; Tada *et al.* 2003). Portions of western and central Cuba were originally attached to Yucatan at the end of the Cretaceous, and later translated from the SW Maya/Yucatan block and juxtaposed against the Bahamas–Cuba–Florida Platform during later Cenozoic emplacement of the Caribbean Plate (Ascanio-Pellon *et al.* 2022).

Basin palaeobathymetry uncertainty

Estimates of Maastrichtian palaeobathymetry in the Gulf of Mexico can be inferred in onshore, nearshore and shelf depofacies by analogy to modern bathymetric profiles. For example, coeval marine shelves extending out to the relict carbonate shelf margin were probably similar to modern neritic water depths with a maximum of 200± metres. However, deep marine systems are less well constrained due to the wide range of abyssal plain depths observed in nature. For ancient systems like that of the Cretaceous, depth zones of benthic foraminifera are calibrated against independent palaeodepth estimates (e.g. Berggren and Aubert 1975; Berggren and Miller 1989; Alegret *et al.* 2001). We use ecological zones based on microfauna and microflora (especially nannofossils) in well cuttings to estimate palaeowater depths.

Five key wells in the northern Gulf of Mexico tested the Late Cretaceous and/or the K–Pg boundary unit in the deep Gulf of Mexico Basin outside of the relict shelf margin (Table 2). The BP operated Tiber #1 well of the Keathley Canyon protraction Block 102 (well location 17 in Fig. 4) penetrated the Cretaceous from K–Pg boundary to the well total depth (TD) in Ceno-Turonian (Fig. 13; Sweet *et al.* 2022). About 85 m (280 ft) of light-grey coloured, finely crystalline (micritic) limestone represents the K–Pg boundary unit (Denne *et al.* 2013; Scott *et al.* 2014). Below that unit are 238 m (780 ft) of pre-impact Cretaceous strata ranging in age from Maastrichtian to Campanian, which, in turn, unconformably overlie Cenomanian–Turonian shales (Eagle Ford equivalent). Biostratigraphic reports from the wellsite interpret the palaeobathymetry as Ecological Zone (Ecozone) 4 (Upper Bathyal, 200–500 m palaeowater depth) in the K–Pg boundary unit, and Ecozone 5 (Middle Bathyal, 500–2000 m palaeowater depth) in the pre-impact section.

The Baha II (Alaminos Canyon Block 557#1) well, located to the SW (well location 18 in Fig. 4), shows a similar palaeowater range depth (Middle Bathyal Ecozone 5; Table 2) from limestones and chalks below the 300 m (980 ft) thick K–Pg boundary unit. As with the Tiber well, this palaeobathymetric estimate is based on wellsite microfossils and microflora (Denne *et al.* 2013).

Onshore wells (Highlander, Jeanerette Minerals LLC #1, St. Martin Parish, Louisiana; well location

Table 2. Palaeobathymetric estimates for GoM Deep wells at Top Cretaceous (or K–Pg boundary unit)

Well	Top K–Pg boundary unit	Top Cretaceous	Ecozone	Comments
Tiber (Keathley Canyon 102 #1) Figure 5: Well 17	32 330 ft	32 611 ft MD (Denne *et al.* 2013)	Ecozone 5-Middle Bathyal	(1500 to 3600 ft; 457 to 1097 m WD in modern seas)*
Highlander (Jeanerette Minerals LLC#1, St. Martin Parish, Louisiana; onshore) Figure 5: Well 20	Top K–Pg at 27 560 ft; in K–Pg at 27 590 ft MD	In Cretaceous (Maastrichtian?) at 27 600 ft MD	Ecozone 4-Upper Bathyal (Upper slope) at 27 590–27 640 ft MD	Shallows to Ecozone 3 (outer shelf, 100–200 m WD) at 28 010 ft MD- in Coniacian; Ecozone 3 (outer shelf, 100–200 m WD) continues to 28 010 ft MD: palaeotransport of shallower water fauna possible†
Baha II (Alaminos Canyon 557 #1) Figure 5: Well 18	Top K–Pg 16 600 ft	Base K–Pg/Top Campanian 17 230 ft	Ecozone 5-Middle Bathyal (1500–2000 m palaeo-WD*) from Paleocene to TD	Chalks and limestones in pre-impact section
Main Pass 295-1 Figure 5: Well 21	Top K–Pg 18 385 ft TVD	Cenomanian below base K–Pg, 18 400 ft TVD	Ecozone 3/4 border at 18 780 ft MD	100 to 500 m palaeo-WD*
Shenandoah #4 (Walker Ridge 51 ST01BP01, API 608124010102) Figure 5: Well 19	32 354 ft TVD	Base K–Pg 31 388 ft TVD; reported as marls and limestones below to TD at 31 591.6 ft TVD	Ecozone 5.5, which in modern oceans is 2000–4500 ft deep*	Cored K–Pg in Core Six; 29 ft of fractured micrite and calcarenites; some out of place Turonian nannos; Campanian to TD‡

Abbreviations: GoM, Gulf of Mexico; K–Pg, Cretaceous Paleogene boundary; WD, water depth; MD, measured depth; TVD, true vertical depth; ecozone, ecological zone.
Source: *Mesozoic oceans could be deeper due to higher salinity (R. Weber, pers. comm. 2023); †M. Purkey Phillips (pers. comm. 2022); ‡R. Denne (pers. comm. 2022).

20 in Fig. 4) and nearshore wells (Main Pass 295-1, well location 21 in Fig. 4) are interpreted as ranging in palaeowater depths of upper slope to outer shelf (Ecozones 3 to 4; 100 to 500 m palaeowater depth). This is shallower palaeobathymetry than Tiber and Baha II but still quite deep in palaeowater depths relative to updip locations (e.g. Justiss #1 IPHN Central well, north Louisiana; well location 13 in Fig. 4).

These well-based palaeowater depth estimates are consistent with several other deep basin wells, yet somewhat in conflict with a study of Campanian outcrops that suggested palaeowater depths exceeding 1000 m in the Mississippi embayment as far north as the Arkansas–Louisiana state line (Ebersole 2009). As this would be deeper than wells described closer to the centre of the Gulf of Mexico Basin, one must conclude that Ebersole (2009) made an overestimate due to a questionable method of using well depth as a palaeobathymetric indicator.

Our view is that Maastrichtian palaeowater depths probably mirror the general trend of structural depths geometrically (e.g. steeper gradients seaward of the shelf margin, flattening over oceanic crust, etc.; Fig. 9). But it is highly unlikely that the Late Cretaceous palaeobathymetry ever exceeded Middle Bathyal water depths, as documented in Keathley Canyon and Alaminos Canyon deep basin wells (Table 2).

In any case, however, we envision a substantial depth range from terrestrial to Middle Bathyal palaeoenvironments in the late Maastrichtian of the Gulf of Mexico Basin. The wide range of palaeowater depths is also manifested in the 'complex clastic unit', an interval containing mixed Maastrichtian and Danian faunal and floral assemblages above the K–Pg boundary in sites proximal to the Chicxulub impact site (Arenillas *et al.* 2011) or at considerable distances within the deepwater northern Gulf of Mexico (Denne *et al.* 2013). This juxtaposition of shallow water (e.g. rudist breccias) and deepwater (e.g. bathyal turbidities) indicators is a common occurrence in Mexico, where tectonically enhanced steep gradients from land to deep basin were prominent (Lawton *et al.* 2020). The erosional gaps at the K–Pg boundary in many localities point to significant reworking and redeposition of material from a broad range of water depths (Arz *et al.* 2022).

Uncertain connection between the Gulf of Mexico and the Pacific Ocean

An additional uncertainty in our depositional palaeogeography is the location of a potential Maastrichtian connection between the Gulf of Mexico and the Pacific Ocean, north of the Central American Seaway between North and South America (Fig. 1). One potential pathway would be through the area NW of the Chiapas Massif, where oceanic crust potentially comes onshore near Veracruz (north of location 5 in Fig. 4). This is a problematic area due to post-Cretaceous tectonics (Chiapanecan orogeny) and limited well control.

Outcrops of Maastrichtian strata in Mexico, Belize and Guatemala may shed some light on this question (Fig. 10, red-filled squares). A well-known K–Pg boundary outcrop called Bochil (location 5 in Figs 3 & 4) is located 600 km SSE of the Chicxulub crater centre, and is much closer to the potential Gulf of Mexico–Pacific Ocean connection. The Bochil outcrop (Fig. 14) is considered a relatively complete section of the late Maastrichtian and early Danian (Stinnesbeck *et al.* 2004; Grajales-Nishimura *et al.* 2000). The post-impact section contains a upward-fining sequence from carbonate breccia to sandstones to micritic mudstones (Montanari *et al.* 1994). The sandstone to mudstone sequence underlies an iridium-rich layer. The thick limestone breccia has a sharp contact with underlying, grey-coloured pelagic limestones and calcarenites of probable Cretaceous age, based on the miliolid *Muricella sp*. Montanari *et al.* (1994) interpret the limestone breccia as the product of a tsunami triggered by the bolide impact on Yucatan. The rudist breccia was thus probably derived from erosion of a marine shelf and *in situ* rudist bank, or a broad shelfal marine area. The presence of sandstones above the breccia could imply proximity to an adjacent barrier shoreline with tidal inlets limiting tsunami marine flooding to the west and enhancing easterly return flows. This is a similar transport process to that inferred for the Upper Escondido sandstones at the Tom Walsh–Owen Field area (Kinsland and Snedden 2016; Snedden and Galloway 2019) and in the La Popa Basin (Lawton *et al.* 2005).

The presence of a continuous shore zone system, from which these sandstones are likely derived, would not support the notion of a connection between the Gulf of Mexico and the Pacific Ocean, at least not in this area. In addition, the development of a Maastrichtian foreland basin on the south flank of the Gulf of Mexico Basin, adjacent to an arc–continent collisional margin (Fig. 8; Pindell *et al.* 1988; Pindell and Barrett 1990), provides strong evidence for a topographic barrier that prevented a Gulf–Pacific marine connection at the time of the K-Pg impact on the Maya block. Study of other outcrops in Chiapas and adjacent areas might yield new insights requiring modification of our reconstruction but this would require unequivocal evidence of a marine connection such as Pacific affinity micro- or macrofossils.

Summary

Our Maastrichtian palaeogeographical reconstruction depicts the Gulf of Mexico just prior to the

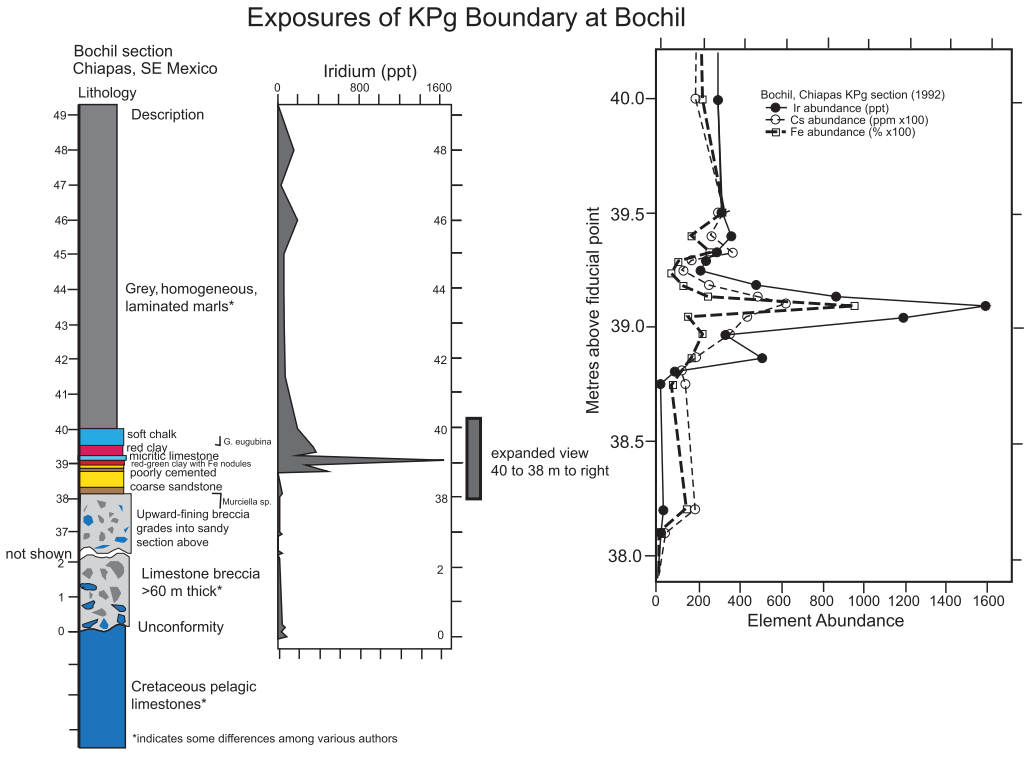

Fig. 14. Bochil outcrop description and iridium measurements. Source: modified from Montanari *et al.* (1994); Arz *et al.* (2022).

Chicxulub impact (Figs 10 & 11). The geographical distribution of palaeoenvironments helps to explain the composition and depositional setting of the K–Pg breccia unit encountered in outcrops and offshore well penetrations. By our synthesis and mapping, Maastrichtian shallow to deep marine carbonate-prone palaeoenvironments represent about 96% of the 2930 km^2 area present at the time of the Chicxulub impact (Fig. 15). Fluvial to shallow marine sandstones amount to just 115 km^2 of the area mapped, excluding limited areas of non-deposition or erosion. In deepwater wells, the dominant lithology of the K–Pg breccia is that of pelagic carbonates (Denne *et al.* 2013), derived from just 33% of the depositional area mapped (Sanford *et al.* 2016), suggesting that reconfiguration of the deep marine seascape was substantial, and attenuation of seismic waves and tsunamis on the shallow shelf did limit, to some degree, the generation of local debris flows. In shallow water areas near the Chicxulub crater, carbonate breccia are similar to shallow marine carbonates of the Maastrichtian–Campanian Yucatan Group of Mexico and equivalents like the Barton Creek and those of Belize (Rodríguez-Tovar *et al.* 2022).

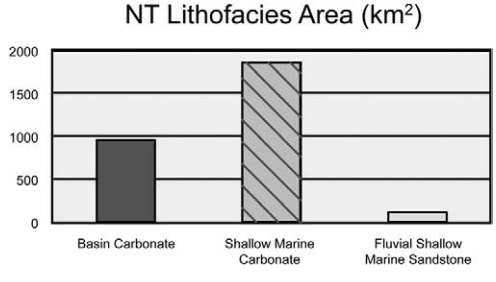

Fig. 15. Depositional area comparisons for the Maastrichtian Stage in the Gulf of Mexico Basin (derived from depositional palaeogeography maps; Figs 10 & 11). Abbreviations: NT, Navarro–Taylor supersequence. Source: from Snedden and Galloway (2019).

The presence of acoustically hard, high compressional velocity carbonates relative to surrounding shales also explains the large impedance contrast and high amplitude seismic response in the subsurface of large areas of the deep Gulf of Mexico Basin (Denne *et al.* 2013). Outside of poorly imaged salt canopies and complex diapirs, the K–Pg

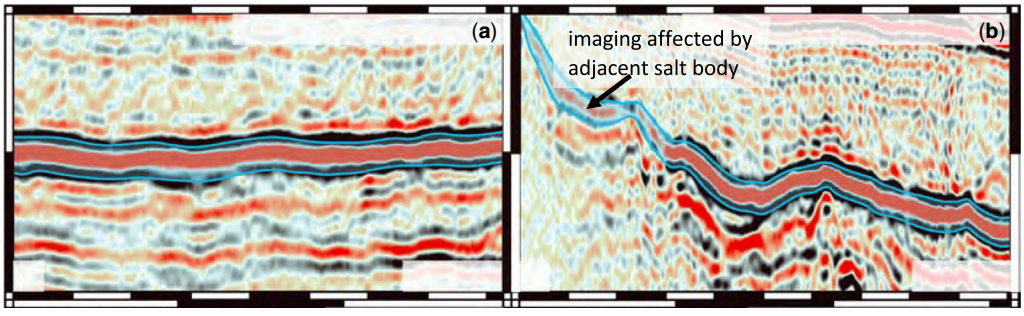

Fig. 16. Examples of K–Pg boundary deposit 2D seismic response. Scale bars are in 1 km intervals; vertical exaggeration (VE) is annotated. Seismic facies of the K–Pg boundary unit in the Gulf of Mexico. (**a**) Characteristic 'blanket' facies in the deepwater gulf, where not occluded by overlying salt or complicated by interacting salt; top and base are both defined by high-amplitude peaks, and the internal character is a uniform, high-amplitude trough with a subtle subjacent stratal truncation. (**b**) Similar to (a) but with more severe truncation of underlying strata and thinning onto adjacent salt ridge (arrow). Source: modified from Snedden and Galloway (2019).

boundary deposit is one of the most continuous and easily mapped seismic horizons in the Gulf of Mexico Basin (Fig. 16; Sanford *et al.* 2016).

Surprisingly, the Late Cretaceous carbonate volumes for the northern Gulf of Mexico K–Pg boundary unit exceed that of the Albian acme of carbonate platform margin development (Snedden and Galloway 2019). Marine flooding of the Mississippi embayment due to global sea level rise and locally diminished siliciclastic input to deltas and shore zones played a role in the expansion of carbonates, despite the closed connection to the Cretaceous WIS in the Maastrichtian.

Effects of the bolide impact event also extend to areas outside of the Gulf of Mexico, in northern South America (e.g. Albertão and Martins 1996; MacLeod *et al.* 2007) and across the globe (Schulte *et al.* 2010). However, the configuration of the areas proximal to the Chicxulub crater influenced processes that propagated outward through the Gulf of Mexico Basin, and with global atmospheric circulation of impact ejecta, left a mark throughout the sedimentary record of the seven continents.

Conclusions

Our understanding of the Cretaceous system, first defined 2 centuries ago by Jean d'Omalius d'Halloy solely from outcrops in France, is greatly enhanced by continued scientific research as well as subsurface exploration in search of economic minerals and fuels. Among the seminal advances in knowledge is recognition of the Chicxulub impact event that ended the Cretaceous, distributing materials from the crater globally and greatly changing the Gulf of Mexico Basin, where the bolide landed. The deep time archive of this basin allows us to reconstruct the depositional palaeogeography and lithological substrate of the late Maastrichtian just prior to this Earth-changing moment. A robust restoration of the palaeoenvironments, bathymetry, sandstone and carbonate content, sea level and ocean circulation is therefore of great importance for realistic modelling of the processes, distribution and composition of the Chicxulub impact products. Our late Maastrichtian depositional palaeogeography is founded on a comprehensive database of wells and reflection seismic data as well as synthesis of information from outcrop studies and prior global plate reconstructions.

(1) The Maastrichtian and earliest Danian Stage was a time of globally high sea level, flooding the Gulf of Mexico Basin and adjacent Mississippi embayment, with widespread deposition of deepwater chalks and shallow marine carbonates. However, connection to the WIS was severed by the tectonics of the nascent Rockies, leaving just the oceanic passages to the Atlantic through the Florida straits. An equatorial seaway separating North and South America (the Central American Seaway) was likely located south of the basin boundary at the Chuacús complex.

(2) Stratigraphic correlations of wells and outcrops illustrate the range of palaeoenvironments from fluvial/coastal plain to deep marine. Siliciclastic input to the basin was largely restricted to a small number of drainage systems, the palaeo-Rio Grande of Texas and New Mexico, the palaeo-Red River of north Texas and Louisiana and shore zones fed by a possible forerunner of the Mississippi River in the northeastern Gulf of Mexico. In onshore Mexico, a laterally continuous wave-

dominated shore zone from the Burgos Basin to Belize is mapped, based upon numerous outcrops of K–Pg boundary sandstones derived from this shoreline. Steep gradients in palaeowater depths probably developed along highly subsiding foreland basins like in the Veracruz area and the Chuacús Complex of central Guatemala, where bathyal turbidites mixed with shallow water limestone breccia.

(3) However, the largest portion of the basin in our reconstruction is covered by marine environments suitable for carbonate production under warming global palaeotemperatures, limited influx of mud and circulation of ocean and shelf currents connected to the world ocean. Continuing a pattern that began in the Early Cretaceous, a tremendous thickness of carbonates accumulated in the basin, with accommodation space provided by salt deflation, palaeophysiography (steep shelf to basin gradients particularly in Mexico) and subsidence. As much as 2000 ft (610 m) of Maastrichtian and Campanian section is mapped over large areas of the basin using subsurface data.

(4) Our maps also explain the dominance of carbonate breccia in the K–Pg boundary unit over the basin, except where locally reduced along pre-existing transform boundaries (Tamaulipas transform). Carbonates probably covered 96% of the Gulf of Mexico Basin, and less than 4% of the area was likely occupied by a siliciclastic system, a distribution that evolved from in the Early Cretaceous. Sandstones in the K–Pg tend to be thin (10 m or less) v. the substantial thicknesses of carbonate breccia and chalks (often more than 30 to 150 m; 100 to 500 ft). The presence of thick, laterally extensive carbonate beds within the K–Pg boundary unit is consistent with the large impedance contrast and high amplitude seismic response of this horizon, mappable over a large portion of the basin.

Acknowledgements The authors gratefully acknowledge contributions from, or discussions with, the following researchers: Mike Sweet (UT-Austin Institute for Geophysics). Assistance by Tim Whiteaker (UT-Austin Institute for Geophysics) and Sean Gulick (UT-Austin Institute for Geophysics) is gratefully acknowledged. Catherine Ross shared her work in progress on the Mexico outcrops and previous detrital zircon U–Pb results from the south Texas well. James Pindell is thanked for his thoughts on the 70 Myr restoration of southern Mexico and for permission to use a figure from his 2023 paper. Chris Scotese is acknowledged for permission to use two reconstructions from his palaeomap atlas. We also gratefully appreciate the reviews by anonymous Reviewer 1 and Richard Denne.

Competing interests The authors declare that they have no known competing financial interests or personal relationships that could have appeared to influence the work reported in this paper.

Author contributions **JWS**: conceptualization (lead), data curation (lead), formal analysis (lead), funding acquisition (lead), writing – original draft (lead); **CML**: validation (lead), writing – review & editing (lead); **TFL**: methodology (lead), validation (equal), writing – review & editing (equal).

Funding The Industrial Associate Members of the Gulf of Mexico Basin Depositional Synthesis Research Project at the University of Texas at Austin funded this research.

Data availability statement All data generated or analysed during this study are included in this published article, except for company proprietary 2D reflection seismic data.

References

Albertão, G.A. and Martins, P.P. 1996. A possible tsunami deposit at the Cretaceous–Tertiary boundary in Pernambuco, northeastern Brazil. *Sedimentary Geology*, **104**, 189–201, https://doi.org/10.1016/0037-0738(95)00128-x

Alegret, L., Molina, E. and Thomas, E. 2001. Benthic foraminifera at the Cretaceous–Tertiary boundary around the Gulf of Mexico. *Geology*, **29**, 891–894, https://doi.org/10.1130/0091-7613(2001)029%3C0891:BFATCT%3E2.0.CO;2

Alvarez, L.W., Alvarez, W., Asaro, F. and Michel, H.V. 1980. Extraterrestrial cause for the Cretaceous–Tertiary extinction. *Science (New York, NY)*, **208**, 1095–1108, https://doi.org/10.1126/science.208.4448.1095

Alzaga-Ruiz, H., Michel, H., Loure, F. and Seranne, M. 2009. Interactions between the Laramide Foreland and the passive margin of the Gulf of Mexico: tectonics and sedimentation in the Golden Lane area, Veracruz state, Mexico. *Marine and Petroleum Geology*, **26**, 951–973, https://doi.org/10.1016/j.marpetgeo.2008.03.009

Aquino-Alberto, G. 2010. *Estudio de Núcleos de Roca del Activo Integral Cantarell de la Sonda de Campeche*. MS thesis, Universidad Nacional Autónoma de México.

Arenillas, I., Arz, J.A. *et al*. 2006. Chicxulub impact event is Cretaceous/Paleogene boundary in age: new micropaleontological evidence. *Earth and Planetary Science Letters*, **249**, 241–257, https://doi.org/10.1016/j.epsl.2006.07.020

Arenillas, I., Arz, J.A. *et al*. 2011. Integrated stratigraphy of the Cretaceous–Tertiary boundary transition in the Gulf of Mexico region: key horizons for hydrocarbon oil exploration. *Gulf Coast Association of Geological Societies Transactions*, **61**, 33–43, https://store.beg.utexas.edu/38-gcags?p=2

Arenillas, I., Arz, J.A., Meléndez, A., Grajales-Nishimura, J. and Rojas-Consuegra, R. 2016. The Chicxulub impact is synchronous with the planktonic foraminifera mass extinction at the Cretaceous/Paleogene boundary: new evidence from the Moncada section, Cuba. *Geologica Acta*, **14**, https://doi.org/10.1344/GeologicaActa2016.14.1.4

Arz, J.A., Arenillas, I., Soria, A.R., Alegret, L., Grajales-Nishimura, J.M., Liesa, C.L. and Rosales, M.C. 2001. Micropaleontology and sedimentology across the Cretaceous/Tertiary boundary at La Ceiba (Mexico): impact-generated sediment gravity flows. *Journal of South American Earth Sciences*, **14**, 505–519, https://doi.org/10.1016/s0895-9811(01)00049-9

Arz, J.A., Alegret, L. and Arenillas, I. 2004. Foraminiferal biostratigraphy and paleoenvironmental reconstruction at the Yaxcopoil-1 drill hole, Chicxulub crater, Yucatán Peninsula. *Meteoritics and Planetary Science*, **39**, 1099–1111, https://doi.org/10.1111/j.1945-5100.2004.tb01131.x

Arz, J.A., Arenillas, I. *et al*. 2022. No evidence of multiple impact scenario across the Cretaceous/Paleogene boundary based on planktic foraminiferal biochronology. *Geological Society of America Special Papers*, **557**, 415–448, https://doi.org/10.1130/2022.2557(20)

Ascanio-Pellon, P., Stockli, D.F., Ruiz Arriaga, D. and Stockli, L.D. 2022. Detrital zircon provenance study of siliciclastic strata in western and central Cuba: implications for Caribbean tectonics. *Second International Meeting for Applied Geoscience and Energy*, 26–29 August 2022, Houston, USA. Society of Exploration Geophysicists and the American Association of Petroleum Geologists, Abstracts, 2444–2448, https://doi.org/10.1190/image2022-3733784.1

Berggren, W.A. and Aubert, J. 1975. Paleocene benthonic foraminiferal biostratigraphy, paleobiogeography and paleoecology of Atlantic–Tethyan regions: midway-type fauna. *Palaeogeography, Palaeoclimatology, Palaeoecology*, **18**, 73–192, https://doi.org/10.1016/0031-0182(75)90025-5

Berggren, W.A. and Miller, K.G. 1989. Cenozoic bathyal and abyssal calcareous benthic foraminiferal zonation. *Micropaleontology*, **35**, 308–320, https://doi.org/10.2307/1485674

Blum, M. and Pecha, M. 2014. Mid-Cretaceous to Paleocene North American drainage reorganization from detrital zircons. *Geology*, **42**, 607–610, https://doi.org/10.1130/G35513.1

Boettcher, S.S. and Milliken, K.L. 1994. Mesozoic–Cenozoic unroofing of the southern Appalachian Basin: apatite fission track evidence from Middle Pennsylvanian sandstones. *Journal of Geology*, **102**, 655–668, https://doi.org/10.1086/629710

Bottjer, D.J. 1981. Structure of Upper Cretaceous chalk benthic communities, southwestern Arkansas. *Palaeogeography, Palaeoclimatology, Palaeoecology*, **34**, 225–256, https://doi.org/10.1016/0031-0182(81)90066-3

Bottjer, D.J. 1986. Campanian–Maastrichtian chalks of southwestern Arkansas: petrology, paleoenvironments and comparison with other North American and European chalks. *Cretaceous Research*, **7**, 161–196, https://doi.org/10.1016/0195-6671(86)90015-7

Bourgeois, J., Hansen, T.A., Wiberg, P.L. and Kauffman, E.G. 1988. A tsunami deposit at the Cretaceous–Tertiary boundary in Texas. *Science (New York, NY)*, **241**, 567–570, https://doi.org/10.1126/science.241.4865.567

Bralower, T.J., Paull, C.K. and Mark Leckie, R. 1998. The Cretaceous–Tertiary boundary cocktail: Chicxulub impact triggers margin collapse and extensive sediment gravity flows. *Geology*, **26**, 331–334, https://doi.org/10.1130/0091-7613(1998)026%3C0331:TCTBCC%3E2.3.CO;2

Bralower, T.J., Cosmidis, J. *et al*. 2020. Origin of a global carbonate layer deposited in the aftermath of the Cretaceous–Paleogene boundary impact. *Earth and Planetary Science Letters*, **548**, article 116476, https://doi.org/10.1016/j.epsl.2020.116476

Carvajal, C.R. and Steel, R.J. 2006. Thick turbidite successions from supply dominated shelves during sea-level highstand. *Geology*, **34**, 665–668, https://doi.org/10.1130/G22505.1

Claeys, P., Kiessling, W. and Alvarez, W. 2002. Distribution of Chicxulub ejecta at the Cretaceous-Tertiary boundary. *Geological Society of America Special Paper*, **356**, 55–68, https://doi.org/10.1130/0-8137-2356-6.55

Coates, A.G., Jackson, J.B.C. *et al*. 1992. Closure of the Isthmus of Panama. The near-shore marine record of Costa Rica and western Panama. *Geological Society of America Bulletin*, **104**, 814–828, https://doi.org/10.1130/0016-7606(1992)104<0814:COTIOP>2.3.CO;2

Cooper, J.D. 1973. Cretaceous–Tertiary transition: Rio Grande outcrop section. *American Journal of Science*, **273**, 431–443.

Cunningham, R., Phillips, M.P. *et al*. 2022. Productivity and organic carbon trends through the Wilcox Group in the deep Gulf of Mexico: evidence for ventilation during the Paleocene-Eocene Thermal Maximum. *Marine and Petroleum Geology*, **140**, https://doi.org/10.1016/j.marpetgeo.2022.105634

Denne, R.A. 2007. Paleogene calcareous nannofossil bioevents from the fold belts of the deep-water central Gulf of Mexico. *In*: Rosen, N. (ed.) *The Paleogene of the Gulf of Mexico and Caribbean Basins: Processes, Events, and Petroleum Systems*. GCSSEPM 27th Annual Research Conference, 2–5 December, Houston, USA, https://doi.org/10.5724/gcs.07.27.0211

Denne, R.A. and Blanchard, R.H. 2013. Regional controls on the formation of the ancestral DeSoto Canyon by the Chicxulub impact. *Gulf Coast Association of Geological Societies Journal*, **2**, 17–28.

Denne, R.A., Scott, E.D., Eickhoff, D.P., Kaiser, J.S., Hill, R.J. and Spaw, J.M. 2013. Massive Cretaceous–Paleogene boundary deposit, deep-water Gulf of Mexico: new evidence for widespread Chicxulub-induced slope failure. *Geology*, **41**, 983–986, https://doi.org/10.1130/G34503.1

Drake, W.R. and Hawkins, S.J. 2021. Sequence stratigraphy of the Niobrara Formation: implications for age-constraining tectonic events and stratigraphic complexities in the Denver–Julesburg Basin, United States. *American Association of Petrolemum Geologists Bulletin*, **105**, 1293–1328, https://doi.org/10.1306/12092019098

Ebersole, S.M. 2009. *Biostratigraphy, Paleogeography, and Paleoenvironments of the Upper Cretaceous (Campanian) Northern Mississippi Embayment*. PhD thesis, The University of Alabama.

Eguiluz de Antuñano, S. 2001. Geologic evolution and gas resources of the Sabinas Basin in northeastern Mexico. *American Association of Petroleum Geologists Memoirs*, **75**, 241–270.

Ewing, T.E. and Lopez, R.F. 1991. Principal structural features, Gulf of Mexico Basin, plate 2. *In*: Salvador, A. (ed.) *The Geology of North American Geological Society of America*. Boulder, Colorado.

Filina, I. and Beutel, E. 2022. Geological and geophysical constraints guide new tectonic reconstruction of the Gulf of Mexico [Preprint]. *Authorea*, https://doi.org/10.1002/essoar.10511463.1

Filina, I., Austin, J. *et al.* 2021. Opening of the Gulf of Mexico: what we know, what questions remain, and how we might answer them. *Tectonophysics*, **822**, article 229150, https://doi.org/10.1016/j.tecto.2021.229150

Fitz-Díaz, E., van der Pluijm, B., Hudleston, P. and Tolson, G. 2014. Progressive, episodic deformation in the Mexican Fold-Thrust Belt (central Mexico): evidence from isotopic dating of folds and faults. *International Geology Review*, **56**, 734–755, https://doi.org/10.1080/00206814.2014.896228

Fitz-Díaz, E., Lawton, T.F., Juárez-Arriaga, E. and Chávez-Cabello, G. 2018. The Cretaceous–Paleogene Mexican orogen: structure, basin development, magmatism and tectonics. *Earth-Science Reviews*, **183**, 56–84, https://doi.org/10.1016/j.earscirev.2017.03.002

Gale, A.S., Mutterlose, J., Batenburg, S., Gradstein, F.M., Agterberg, F.P., Ogg, J.G. and Petrizzo, M.R. 2020. The Cretaceous Period. *In*: Gradstein, F., Ogg, J., Schmitz, M. and Ogg, G.M. (eds) *Geologic Time Scale 2020*. ScienceDirect, 1023–1086, https://doi.org/10.1016/B978-0-12-824360-2.00027-9

Galloway, W.E., Whiteaker, T.L. and Ganey-Curry, P. 2011. History of Cenozoic North American drainage basin evolution, sediment yield, and accumulation in the Gulf of Mexico basin. *Geosphere*, **7**, 938–973, https://doi.org/10.1130/GES00647.1

Geological Society of America 2022. *Timescale v. 6.0*. Geological Society of America, https://www.geosociety.org/GSA/GSA/timescale/home.aspx [last accessed 5 October 2023].

Gilabert, V., Arz, J.A., Arenillas, I., Robinson, S.A. and Ferrer, D. 2021. Influence of the latest Maastrichtian Warming Event on planktic foraminiferal assemblages and ocean carbonate saturation at Caravaca, Spain. *Cretaceous Research*, **125**, article 104844, https://doi.org/10.1016/j.cretres.2021.104844

Gradstein, F.M., Ogg, J.G., Schmitz, M.D. and Ogg, G.M. (eds) 2020. *Geologic Time Scale 2020*. Elsevier, Amsterdam.

Grajales-Nishimura, J.M., Cedillo-Pardo, E. *et al*. 2000. Chicxulub impact: the origin of reservoir and seal facies in the southeastern Mexico oil fields. *Geology*, **28**, 307–310, https://doi.org/10.1130/0091-7613(2000)28<307:CITOOR>2.0.CO;2

Gulick, S.P.S., Christeson, G.L., Barton, P.J., Grieve, R.A.F., Morgan, J.V. and Urrutia-Fucugauchi, J. 2013. Geophysical characterization of the Chicxulub impact crater. *Review of Geophysics*, **51**, 31–52, https://doi.org/10.1002/rog.20007

Gulick, S.P.S., Bralower, T.J., *et al*. 2019. The first day of the Cenozoic. *Proceedings of the National Academy of Sciences*, **116**, 19342–19351, https://doi.org/10.1073/pnas.1909479116

Guzman-Hidalgo, E., Grajales-Nishimura, J.M., Eberli, G.P., Aguayo-Camargo, J.E., Urrutia-Fucugauchi, J. and Perez-Cruz, L. 2021. Seismic stratigraphic evidence of a pre-impact basin in the Yucatán Platform: morphology of the Chicxulub crater and K/Pg boundary deposits. *Marine Geology*, **441**, article 106594, https://doi.org/10.1016/j.margeo.2021.106594

Hancock, J.M. and Kaufman, E.G. 1979. The great transgressions of the Late Cretaceous. *Journal of the Geological Society*, **136**, 175–186, https://doi.org/10.1144/gsjgs.136.2.0175

Haq, B.U. and Shutter, S.R. 2008. A chronology of Paleozoic sea-level changes. *Science (New York, NY)*, **322**, 64–68, https://doi.org/10.1126/science.1161648

Hardenbol, J., Thierry, J., Farley, M.B., Jacquin, T., De Graciansky, P.-C. and Vail, P.T. 1998. Mesozoic and Cenozoic sequence chronostratigraphic framework of European basins. *SEPM Special Publications*, **60**, 3–14.

Hart, M.B., Yancey, T.E., Leighton, A.D., Miller, B., Liu, C., Smart, C.W. and Twitchett, R.J. 2012. The Cretaceous–Paleogene boundary in the Brazos River, Texas: new stratigraphic sections and revised interpretations. *GCAGS Journal*, **1**, 69–80.

Hart, M.B., Harries, P.J. and Cardenas, A.L. 2013. The Cretaceous/Paleogene boundary events in the Gulf Coast: comparisons between Alabama and Texas. *Gulf Coast Association of Geological Societies Transactions*, **63**, 235–255.

Heine, C., Yeo, L.G. and Müller, R.D. 2015. Evaluating global paleoshoreline models for the Cretaceous and Cenozoic. *Australian Journal of Earth Sciences*, **62**, 275–287, https://doi.org/10.1080/08120099.2015.1018321

Hildebrand, A.R., Penfield, G.T., Kring, D.A., Pilkington, M., Camargo, Z.A., Jacobsen, S.B. and Boynton, W.V. 1991. Chicxulub crater: a possible Cretaceous/Tertiary boundary impact crater on the Yucatan Peninsula, Mexico. *Geology*, **19**, 867–871, https://doi.org/10.1016/j.earscirev.2020.103463

Hübscher, C., Häcker, T., Betzler, C., Kalvelage, C. and Benedikt, W. 2023. Reading the sediment archive of the eastern Campeche Bank (southern Gulf of Mexico): from the aftermath of the Chicxulub impact to Loop Current variability. *Marine Geophysical Research*, **44**, https://eartharxiv.org/repository/view/4995/29pp

Hudec, M.R., Jackson, M.P. and Peel, F.J. 2013. Influence of deep Louann structure on the evolution of the northern Gulf of Mexico. *American Association of Petroleum Geologists Bulletin*, **97**, 1711–1735, https://doi.org/10.1306/04011312074

Hull, P.M., Bornemann, A., Penman, D.E., Henehan, M.J., Norris, R.D., Wilson, P.A. and Zachos, J.C. 2020. On impact and volcanism across the Cretaceous–Paleogene boundary. *Science (New York, NY)*, **367**, 266–272, https://doi.org/10.1126/science.aay5055

Jackson, M.P.A., Dooley, T.P., Hudec, M.R. and McDonnell, A. 2011. The pillow fold belt: a key subsalt

structural province in the northern Gulf of Mexico. *AAPG Search and Discovery*, https://www.searchanddiscovery.com/pdfz/documents/2011/10329jackson/ndx_jackson.pdf.html [last accessed 22 January 2024].

Jackson, W.T., McKay, M.P., Beebe, D.A., Mullins, C., Ionescue, A. and Shaulis, B. 2021. Late Cretaceous sediment provenance in the eastern Gulf Coastal Plain (U.S.A.) based on detrital zircon U–Pb ages and TH/U values. *Journal of Sedimentary Research*, **91**, 1025–1039, https://doi.org/10.2110/jsr.2020.177

Johnson, C.C. 1999. Evolution of Cretaceous surface current circulation patterns, Caribbean and Gulf of Mexico. *Geological Society of America Special Papers*, **332**, 329–343, https://doi.org/10.1130/0-8137-2332-9.329

Johnston, J.E., III, Heinrich, P.V., Lovelace, J.K., McCulloh, R.P. and Zimmerman, R.K. 2000. Folio series no. 8: Stratigraphic Charts of Louisiana 2000, https://www.lsu.edu/lgs/publications/products/stratigraphic-charts-louisiana.php

Jones, H.L., Lowery, C.M. and Bralower, T.J. 2019. Delayed calcareous nannoplankton boom–bust successions in the earliest Paleocene Chicxulub (Mexico) impact crater. *Geology*, **47**, 753–756, https://doi.org/10.1130/G46143.1

Keller, G., Abramovich, S., Adatte, T. and Berner, Z. 2011. Biostratigraphy, age of Chicxulub impact, and depositional environment of the Brazos River KTB sequences. *SEPM Special Publications*, **100**, 82–122, https://doi.org/10.2110/sepmsp.100.081

Kelly, D.C., Arnold, A.J. and Parker, W.C. 1996. Paedomorphosis and the origin of the Paleogene planktonic foraminiferal genus Morozovella. *Paleobiology*, **22**, 266–281, https://doi.org/10.1017/S0094837300016213

Kennedy, C.J. 2013. *Detrital Zircon U–Pb Ages and Provenance Study of the Late Jurassic Bossier Sands, East Texas Subsurface*. MS thesis, University of Texas at Dallas.

Kinsland, G.L. and Snedden, J.W. 2016. Comparison of a portion of the K/Pg boundary deposits in two locations: Webb County, Texas, and LaSalle Parish, Louisiana. *Gulf Coast Association of Geological Societies Transactions*, **66**, 789–797, http://www.gcags.org/exploreanddiscover/2016/00071_kinsland_and_snedden.pdf

Kocsis, A.T. and Scotese, C.R. 2021. Mapping paleocoastlines and continental flooding during the Phanerozoic. *Earth-Science Reviews*, **213**, article 103463, https://doi.org/10.1016/j.earscirev.2020.103463

Kominz, M.A., Browning, J.V., Miller, K.G., Sugarman, P.J., Mizintseva, S. and Scotese, C.R. 2008. Late Cretaceous to Miocene sea-level estimates from the New Jersey and Delaware coastal plain coreholes: an error analysis. *Basin Research*, **2**, 211–226, https://doi.org/10.1111/j.1365-2117.2008.00354.x

Kornecki, K.M., Feldmann, R.M. and Schweitzer, C.E. 2017. Decapoda (Crustacea) of the Coon Creek Formation (Maastrichtian) of Mississippi and Tennessee. *Florida Museum of Natural History Bulletin*, **53**, 269–334, https://doi.org/10.58782/flmnh.danf1986

Kring, D.A. 2005. Hypervelocity collisions into continental crust composed of sediments and an underlying crystalline basement: comparing the Ries (24 km) and Chicxulub (180 km) impact craters. *Chemie der Erde*, **65**, 1–46, https://doi.org/10.1016/j.chemer.2004.10.003

Kring, D.A. 2007. The Chicxulub impact event and its environmental consequences at the Cretaceous–Tertiary boundary. *Palaeogeography, Palaeoclimatology, Palaeoecology*, **255**, 4–21, https://doi.org/10.1016/j.palaeo.2007.02.037

Lawton, T.F., Vega, F.J., Giles, K.A. and Rosales-Dominguez, C. 2001. Stratigraphy and origin of the La Popa Basin, Nuevo León and Coahuila, Mexico. *American Association of Petroleum Geologists Memoirs*, **75**, 219–240, https://doi.org/10.1306/M757 68C9

Lawton, T.F., Shipley, K.W., Aschoff, J.L., Giles, K.A. and Vega, F.J. 2005. Basinward transport of Chicxulub ejecta by tsunami-induced backflow, La Popa basin, northeastern Mexico, and its implications for distribution of impact-related deposits flanking the Gulf of Mexico. *Geology*, **33**, 81–84, https://doi.org/10.1130/0091-7613-33.1.e86

Lawton, T.F., Bradford, I.A., Vega, F.J., Gehrels, G.E. and Amato, J.M. 2009. Provenance of Upper Cretaceous–Paleogene sandstones in the foreland basin system of the Sierra Madre Oriental, northeastern Mexico, and its bearing on fluvial dispersal systems of the Mexican Laramide Province. *Geological Society of America Bulletin*, **121**, 820–836, https://doi.org/10.1130/B26450.1

Lawton, T.F., Sierra-Rojas, M.I. and Martens, U. 2020. Stratigraphic correlation chart of Carboniferous–Paleogene rocks of Mexico, adjacent southwestern United States, Central America, and Colombia. *Geological Society of America Special Papers*, **546**, 1–28, https://doi.org/10.1130/2020.2546(05)

Lawton, T., Giles, K. and Rowan, M. 2021. *La Popa Basin, Nuevo León and Coahuila, Mexico: Halokinetic Sequences and Diapiric Structural Kinematics in the Field*. Springer.

Leighton, A.D., Hart, M.B., Smart, C.W., Leng, M.J. and Hampton, M. 2017. Timing recovery after the Cretaceous/Paleogene boundary: evidence from the Brazos River, Texas, USA. *Journal of Foraminiferal Research*, **47**, 229–238, https://doi.org/10.2113/gsjfr.47.3.229

Lopez-Ramos, E. 1975. Geological summary of the Yucatan Peninsula. *In*: Nairn, A.E.M. and Stehli, F.G. (eds) *The Gulf of Mexico and the Caribbean*. Springer, 257–282.

Lowery, C.M. and Bralower, T.J. 2022. Elevated post K–Pg export productivity in the Gulf of Mexico and Caribbean. *Paleoceanography and Paleoclimatology*, **37**, article e2021PA004400, https://doi.org/10.31223/X59053

Lowery, C.M., Bralower, T.J. *et al*. 2018. Rapid recovery of life at ground zero of the end-Cretaceous mass extinction. *Nature*, **558**, 288–291, https://doi.org/10.1038/s41586-018-0163-6

Lowery, C.M., Morgan, J.V., Gulick, S.P., Bralower, T.J. and Christeson, G.L. 2019. Ocean drilling perspectives on meteorite impacts. *Oceanography*, **32**, 120–134, https://doi.org/10.5670/oceanog.2019.133

Lowery, C.M., Jones, H.L. *et al*. 2021. Early Paleocene paleoceanography and export productivity in the Chicxulub crater. *Paleoceanography and Paleoclimatology*, **36**, article e2021PA004241, https://doi.org/10.1029/2021PA004241

Luterbacher, H. and Premoli Silva, I. 1964. Biostratigraphy of the Cretaceous–Tertiary boundary in the central Apennines. *Rivista Italiana di Paleontologia e Stratigrafia*, **70**, 67–128.

MacLeod, K.G., Whitney, D.L., Huber, B.T. and Koeberl, C. 2007. Impact and extinction in remarkably complete Cretaceous–Tertiary boundary sections from Demerara Rise, tropical western North Atlantic. *The Geological Society of America Bulletin*, **119**, 101–115, https://doi.org/10.1130/B25955.1

Mahmoud, S. 2004. *Integrated Palynology and Sequence Stratigraphy of the Upper Cretaceous (Maastrichtian) Strata, Rio Grande Embayment, Texas, Using Well, Outcrop, and Seismic Data*. PhD thesis, The University of Texas at Dallas.

Mancini, E.A. 1984. Biostratigraphy of Paleocene strata in southwestern Alabama. *Micropaleontology*, **30**, 268–291, https://doi.org/10.2307/1485690

Mancini, E.A., Tew, B.H. and Smith, C.C. 1989. Cretaceous–Tertiary contact, Mississippi, and Alabama. *The Journal of Foraminiferal Research*, **19**, 93–104, https://doi.org/10.2113/gsjfr.19.2.93

Martens, U.C. and Sierra-Rojas, M.I. 2021. Late Cretaceous–Paleocene transition from calcareous platform to basinal deposition in western Chiapas, Mexico. *GSA Special Papers*, **546**, 171–195, https://doi.org/10.1130/2021.2546(07)

Martens, U.C., Brueckner, H.K., Mattinson, C.G., Liou, J.G. and Wooden, J.L. 2012. Timing of eclogite-facies metamorphism of the Chuacús complex, central Guatemala: record of Late Cretaceous continental subduction of North America's sialic basement. *Lithos*, **146–147**, 1–10, https://doi.org/10.1016/j.lithos.2012.04.021

Martini, E. 1970. Standard Palaeogene calcareous nannoplankton zonation. *Nature*, **226**, 560–561, https://doi.org/10.1038/226560a0

McGowen, M.K. and Lopez, C.M. 1983. *Depositional Systems in the Nacatoch Formation (Upper Cretaceous), Northeast Texas and Southwest Arkansas*. The University of Texas at Austin, Bureau of Economic Geology. Report of Investigations **137**.

Miller, J.G., Kominz, M.A. *et al*. 2005. The Phanerozoic record of global sea-level change. *Science (New York, NY)*, **310**, 1293–1298, https://doi.org/10.1126/science.1116412

Miller, K.G., Browning, J.V., Schmelz, W.J., Kopp, R.E., Mountain, G.S. and Wright, J.D. 2020. Cenozoic sea-level and cryospheric evolution from deep-sea geochemical and continental margin records. *Science Advances*, **6**, article eaaz1346, https://doi.org/10.1126/sciadv.aaz1346

Montanari, A., Claeys, P., Aasaro Bermudez, J. and Smit, J. 1994. Preliminary stratigraphy and iridium and other geochemical anomalies across the KT boundary in the Bochil section (Chiapas, southeastern Mexico). *New Developments Regarding the KT Event and Other Catastrophes in Earth History*, 9–12 February 1994, Houston, USA, Extended Abstracts, https://hdl.handle.net/20.500.11753/1037

Montes, C., Cardona, A. *et al*. 2015. Middle Miocene closure of the Central American Seaway. *Science (New York, NY)*, **348**, 226–229, https://doi.org/10.1126/science.aaa2815

Morgan, J.V., Gulick, S.P., Bralower, T., Chenot, E., Christeson, G., Claeys, P. and Zylberman, W. 2016. The formation of peak rings in large impact craters. *Science (New York, NY)*, **354**, 878–882, https://doi.org/10.1126/science.aah6561

Morgan, J., Gulick, S., Mellett, C.L., Green, S.L. and the Expedition 364 Scientists 2017. Chicxulub: drilling the K–Pg impact crater. Proceedings of the International Ocean Discovery Program, 364, https://doi.org/10.14379/iodp.proc.364.107.2017

Muchiri, E. 2018. *Optical Inspections and Scanning Electron Microscopy across the Cretaceous–Paleogene Boundary Deposit in Well-Core IPNH No. 2 from LaSalle Parish, Central Louisiana*. MS thesis, University of Louisiana at Lafayette.

Murillo-Muneton, G., Grajales-Nishimura, J.M. *et al*. 2002. Stratigraphic architecture and sedimentology of the main oil-producing interval at the Cantarell Oil Field: the K–T boundary sedimentary succession, February 2002, Villahermosa, Mexico, https://doi.org/10.2118/74431-MS

Nederbragt, A.J. 1991. Late Cretaceous biostratigraphy and development of Heterohelicidae (planktic foraminifera). *Micropaleontology*, **37**, 329–372, https://doi.org/10.2307/1485910

Ocampo, A.C. and Pope, K.O. 1994. A KT boundary section from northern Belize. *In*: *New Developments Regarding the KT Event and Other Catastrophes in Earth History*, 9–12 February 1994, Houston, USA, Extended Abstracts, https://ntrs.nasa.gov/api/citations/19940023791/downloads/19940023791.pdf

Ocampo, A.C., Pope, K.O. and Fischer, A.G. 1996. Ejecta blanket deposits of the Chicxulub crater from Albion Island, Belize. *Geological Society of America Special Papers*, **307**, 75–88, https://doi.org/10.1130/0-8137-2307-8.75

O'Dea, A., Lessios, H.A. *et al*. 2016. Formation of the Isthmus of Panama. *Science Advances*, **2**, article e1600883, https://doi.org/10.1126/sciadv.1600883

Olson, H.C., Snedden, J.W. and Cunningham, R. 2015. Development and application of a robust chronostratigraphic framework in Gulf of Mexico Mesozoic exploration. *Interpretation*, **3**, 39–58, https://doi.org/10.1190/INT-2014-0179.1

Olsson, R.K. and Liu, C. 1993. Controversies on the placement of Cretaceous–Paleogene boundary and the K/P mass extinction of planktonic foraminifera. *Palaios*, **8**, 127–139, https://doi.org/10.2307/3515167

Olsson, R.K., Liu, C., Van Fossen, M. and Ryder, G. 1996. The Cretaceous–Tertiary catastrophic event at Millers Ferry, Alabama. *Geological Society of America Special Papers*, **307**, 263–277.

Penfield, G.T. and Camargo-Zanoguera, A. 1981. Definition of a major igneous zone in the central Yucatan Platform with aeromagnetics and gravity. *51st Annual Meeting, Society of Exploration Geophysicists Technical Program, Abstracts and Bibliographies*, Tulsa, USA.

Percival, S.F. and Fischer, A.G. 1977. Changes in calcareous nannoplankton in the Cretaceous–Tertiary biotic crisis at Zumay. *Evolutionary Theory*, **2**, 1–35.

Pessagno, E.A. 1969. Upper Cretaceous stratigraphy of the western Gulf Coast area of Mexico, Texas, and Arkansas. *Geological Society of America Memoirs*, **111**.

Pessagno, E.A., Longoria, J.F., Smith, C.C., Alshuabi, A.A., Thompson, L.B., Graham, J. and Holloway, J.W. 2023. Planktonic foraminiferal zonation and stratigraphy of Cretaceous and Lower Paleogene strata of the western Gulf Coastal Plain and the Caribbean. *Maya Revista de Geociencias*, February, 16–86.

Phelps, R.M., Kerans, C., Loucks, R.G., Da Gama, R., Jeremiah, J. and Hull, D. 2014. Oceanographic and eustatic control of carbonate platform evolution and sequence stratigraphy on the Cretaceous (Valanginian–Campanian) passive margin, northern Gulf of Mexico. *Sedimentology*, **61**, 461–496, https://doi.org/10.1111/sed.12062

Phelps, R.M., Kerans, C., Da-Gama, R.O.B.P., Jeremiah, J., Hull, D. and Loucks, R.G. 2015. Response and recovery of the Comanche carbonate platform surrounding multiple Cretaceous oceanic anoxic events, northern Gulf of Mexico. *Cretaceous Research*, **54**, 117–144, https://doi.org/10.1016/j.cretres.2014.09.002

Pindell, J. and Barrett, S. 1990. Geologic evolution of the Caribbean region: a plate tectonic perspective. *In*: Dengo, G. and Case, J.E. (eds) *The Caribbean Region*. Geological Society of America, Boulder, USA, 405–432, https://doi.org/10.1130/DNAGGNA-H.405

Pindell, J.L., Cande, S.C., Pitman, W.C., III, Rowley, D.B., Dewey, J.F., Labrecque, J. and Haxby, W. 1988. A plate-kinematic framework for models of Caribbean evolution. *Tectonophysics*, **155**, 121–138, https://doi.org/10.1016/0040-1951(88)90262-4

Pindell, J., Maresch, W.V., Martens, U. and Stanek, K. 2011. The Greater Antillean Arc: Early Cretaceous origin and proposed relationship to Central American subduction mélanges: implications for models of Caribbean evolution. *International Geology Review*, **54**, 131–143, https://doi.org/10.1080/00206814.2010.510008

Pindell, J.L., Miranda, E., Cerón, A. and Hernandez, L. 2016. Aeromagnetic map constrains Jurassic–Early Cretaceous synrift, breakup, and rotational seafloor spreading history in the Gulf of Mexico. *In*: Lowery, C.M., Snedden, J.W. and Rosen, N. (eds) *Mesozoic of the Gulf Rim and Beyond: New Progress in Science and Exploration of the Gulf of Mexico Basin*. Transactions of the 35th Annual GCSSEPM Foundation Perkins–Rosen Research Conference, 8–9 December 2016, Houston, USA. Gulf Coast Section Society for Sedimentary Geology (GCSSEPM), 123–153.

Pindell, J., Villagómez, D., Molina Garza, R., Beltrán, A., Stockli, D. and Wildman, M. 2023. Late Cretaceous–Miocene depositional evolution of Chiapas, Mexico: a foreland controlled by collision of Greater Antilles arc and the subsequent relative migration of the Chortís Block. *Gondwana Research*, **113**, 116–143, https://doi.org/10.1016/j.gr.2022.10.016

Poag, C.W. 2022. Bolide impact effects on the West Florida Platform, Gulf of Mexico: end Cretaceous and late Eocene. *Geosphere*, **18**, 1077–1103, https://doi.org/10.1130/GES02472.1

Potter-McIntyre, S.L., Breeden, J.R. and Malone, D.H. 2018. A Maastrichtian birth of the Ancestral Mississippi River system: evidence from the U–Pb detrital zircon geochronology of the McNairy Sandstone, Illinois, USA. *Cretaceous Research*, **91**, 71–79, https://doi.org/10.1016/j.cretres.2018.05.010

Pyles, D.R. and Slatt, R.M. 2000. A high-frequency sequence stratigraphic framework for shallowthrough deep-water deposits of the Lewis Shale and Foxhills Sandstone, Great Divide and Washakie Basins Wyoming. *SEPM Society for Sedimentary Geology*, **20**, 51–57, https://doi.org/10.5724/gcs.00.15.0836

Range, M.M., Arbic, B.K. *et al*. 2022. The Chicxulub impact produced a powerful global tsunami. *AGU Advances*, **3**, article e2021AV000627, https://doi.org/10.1029/2021AV000627

Rodríguez-Tovar, F.J., Kaskes, P. *et al*. 2022. Life before impact in the Chicxulub area: unique marine ichnological signatures preserved in crater suevite. *Scientific Reports*, **12**, article 11376, https://doi.org/10.1038/s41598-022-15566-z

Rogers, R.D., Mann, P., Emmet, P.A. and Venable, M.E. 2007. Colon fold belt of Honduras: evidence for Late Cretaceous collision between the continental Chortis block and intra-oceanic Caribbean arc. *Geological Society of America Special Papers*, **428**, 129–149, https://doi.org/10.1130/2007.2428(06)

Romein, A. 1977. Calcareous nannofossils from Cretaceous–Tertiary boundary interval in Barranco del Gredero (Caravaca, prov-Murcia, SE Spain). *Proceedings of the Koninklijke Nederlandse Akademie van Wetenschappen Series B – Palaeontology Geology Physics Chemistry Anthropology*, **80**, 256–279.

Ross, C., Stockli, D.F. *et al*. 2022. Evidence of Carboniferous arc magmatism preserved in the Chicxulub impact structure. *GSA Bulletin*, **134**, 241–260, https://doi.org/10.1130/B35831.1

Rowan, M.G., Muñoz, J.A., Roca, E., Ferrer, O., Santolaria, P., Granado, P. and Snidero, M. 2022. Linked detachment folds, thrust faults, and salt diapirs: observations and analog models. *Journal of Structural Geology*, **155**, article 104509, https://doi.org/10.1016/j.jsg.2022.104509

Salvador, A. 1991. *The Gulf of Mexico Basin*. Geological Society of America, Boulder, USA.

Sanford, J.C., Snedden, J.W. and Gulick, S.P.S. 2016. The Cretaceous–Paleogene boundary deposit in the Gulf of Mexico: large-scale oceanic basin response to the Chicxulub impact. *Journal of Geophysical Research: Solid Earth*, **121**, 1240–1261, https://doi.org/10.1002/2015JB012615

Schuchert, C. 1955. *Atlas of Paleogeographic Maps of North America*. John Wiley and Sons.

Schulte, P., Alegret, L. *et al*. 2010. The Chicxulub asteroid impact and mass extinction at the Cretaceous–Paleogene boundary. *Science (New York, NY)*, **327**, 1214–1218, https://doi.org/10.1126/science.1177265

Schulte, P., Smit, J., Deutsch, A., Salge, T., Friese, A. and Beichel, K. 2012. Tsunami backwash deposits with Chicxulub impact ejecta and dinosaur remains from the Cretaceous–Palaeogene boundary in the La Popa Basin, Mexico. *Sedimentology*, **59**, 737–765, https://doi.org/10.1111/j.1365-3091.2011.01274.x

Scotese, C.R. 2021. An atlas of Phanerozoic paleogeographic maps: the seas come in and the seas go out. *Annual Review of Earth and Planetary Sciences*, **49**, 679–728, https://doi.org/10.1146/annurev-earth-081320-064052

Scotese, C.R. and Dreher, C. 2012. Global Geology. http://54.189.216.145/GlobalGeology/ [Last accessed 20 February 2023].

Scotese, C.R., Song, H., Mills, B.J.W. and van der Meer, D.W. 2021. Phanerozoic paleotemperatures: the Earth's changing climate during the last 540 million years. *Earth-Science Reviews*, **215**, article 103503, https://doi.org/10.1016/j.earscirev.2021.103503

Scott, E.D., Denne, R.A., Kaiser, J.S. and Eickhoff, D. 2014. Impact on sedimentation into the north-central deepwater Gulf of Mexico as a result of the Chicxulub event. *GCAGS Journal*, **3**, 41–50.

Shellhouse, K. 2017. *The Cretaceous–Paleogene Boundary Deposit in LaSalle Parish, Louisiana*. MS thesis, The University of Louisiana at Lafayette.

Sickmann, Z.T. and Snedden, J.W. 2021. Neogene to recent evolution of the southern Gulf of Mexico Basin: tectonic controls on deep-water sediment dispersal systems. *Basin Research*, **33**, 1240–1265, https://doi.org/10.1111/bre.12512

Sissingh, W. 1977. Biostratigraphy of Cretaceous calcareous nannoplankton. *Geologie en Mijnbouw*, **56**, 37–65.

Smit, J. and Hertogen, J. 1980. An extraterrestrial event at the Cretaceous–Tertiary boundary. *Nature*, **285**, 198–200, https://doi.org/10.1038/285198a0

Smit, J., Roep, T.B., Alvarez, W., Montanari, S. and Claeys, P. 1994. Impact-tsunami-generated clastic beds at the KT boundary of the Gulf Coastal Plain: a synthesis of old and new outcrops. *New Developments Regarding the KT Event and Other Catastrophes in Earth History*, 9–12 February 1994, Houston, USA, Extended Abstracts, https://ntrs.nasa.gov/api/citations/19940023791/downloads/19940023791.pdf

Smit, J., Roep, T.B., Alvarez, W., Montanari, A., Claeys, P., Grajales-Nishimura, J.M. and Bermudez, J. 1996. Coarse-grained, clastic sandstone complex at the K/T boundary around the Gulf of Mexico. Deposition by tsunami waves induced by the Chicxulub impact? *Geological Society of America Special Papers*, **307**, 151–182.

Smith, C.C. and Pessagno, E.A. 1973. Planktonic foraminifera and stratigraphy of the Corsicana Formation (Maestrichtian) north-central Texas. *Cushman Foundation for Foraminiferal Research, Special Publications*, **12**.

Snedden, J.W. 1991. Origin and sequence stratigraphic significance of large dwelling traces in the Escondido Formation (Cretaceous, Texas, USA). *Palaios*, **6**, 541–552, https://doi.org/10.2307/3514917

Snedden, J.W. and Galloway, W.E. 2019. *The Gulf of Mexico Sedimentary Basin. Depositional Evolution and Practical Applications*. Cambridge University Press, https://doi.org/10.1017/9781108292795

Snedden, J.W. and Jumper, R.S. 1990. Shelf and shoreface reservoirs, Tom Walsh–Owen Field, Texas. *In*: Barwis, J.H., McPherson, J.G. and Studlick, J.R.J. (eds) *Sandstone Petroleum Reservoirs. Casebooks in Earth Sciences*. Springer, New York, 415–436.

Snedden, J.W. and Kersey, D.G. 1982. Depositional environments and gas production trends Olmos Sandstone, Upper Cretaceous, Webb County, Texas. *Gulf Coast Association of Geological Societies Transactions*, **32**, 497–518.

Snedden, J.W. and Liu, C. 2011. Recommendations for a uniform chronostratigraphic designation system for Phanerozoic depositional sequences. *American Association of Petroleum Geologists Bulletin*, **95**, 1095–1122, https://doi.org/10.1306/01031110138

Snedden, J.W., Norton, I.O., Christeson, G.L. and Sanford, J.C. 2014. Interaction of deepwater deposition and a midocean spreading center, eastern Gulf of Mexico Basin, USA. *Gulf Coast Association of Geological Societies Transactions*, **64**, 371–383.

Snedden, J.W., Galloway, W.E., Milliken, K.T., Xu, J., Whiteaker, T.L. and Blum, M.D. 2018*a*. Validation of empirical source-to-sink scaling relationships in a continental-scale system: the Gulf of Mexico Cenozoic record. *Geosphere*, **14**, 768–783, https://doi.org/10.1130/GES01452.1

Snedden, J.W., Tinker, L.D. and Virdell, J. 2018*b*. Southern Gulf of Mexico Wilcox source to sink: investigating and predicting Paleogene Wilcox reservoirs in eastern Mexico deep-water areas. *AAPG Bulletin*, **102**, 2045–2074, https://doi.org/10.1306/03291817263

Snedden, J.W., Hull, H.L., Whiteaker, T.L., Virdell, J.W. and Ross, C.H. 2022. Late Mesozoic sandstone volumes recorded in Gulf of Mexico subsurface depocentres: deciphering long-term sediment supply trends and contributions by paleo river systems. *Basin Research*, **34**, 1269–1291, https://doi.org/10.1111/bre.12659

Stinnesbeck, W., Keller, G., Adatte, T., Harting, M., Stuben, D., Istrate, G. and Kramar, U. 2004. Yaxcopoil-1 and the Chicxulub impact. *International Journal of Earth Science (Geol Rundsch)*, **93**, 1042–1065, https://doi.org/10.1007/s00531-004-0431-6

Sweet, M.L., Phillips, M., Snedden, J. and Weber, R. 2022. The Early Cretaceous transition from carbonate to siliciclastic deposition in the deepwater of the northern Gulf of Mexico: new insights from the Keathley Canyon 102#1 well. *GCAGS Journal*, **10**, 58–70, https://www.gcags.org/Journal/2022.GCAGS.Journal/2022_GCAGS_Journal_v10_04_p58-70_Sweet_Et_Al.pdf

Tada, R., Iturralde-Vinent, M.A. *et al*. 2003. K/T boundary deposits in the paleo-western Caribbean Basin. *American Association of Petroleum Geologists Memoirs*, **79**, 582–604, https://doi.org/10.1306/M79877C26

Tantawy, A.A. 2011. Calcareous nannofossils across the Cretaceous–Tertiary boundary at Brazos, Texas, USA: extinction and survivorship, biostratigraphy, and paleoecology. *SEPM Special Publications*, **100**, 157–178, https://doi.org/10.2110/sepmsp.100.157

Thierstein, H.R. and Okada, H. 1979. The Cretaceous/Tertiary boundary event in the North Atlantic. *Initial Reports of the Deep Sea Drilling Project*, **43**, 601–616, http://deepseadrilling.org/43/volume/dsdp43_22.pdf

Tipsword, H.L., Stetzer, F.M. and Smith, F.L., Jr 1966. Interpretation of depositional environment in Gulf Coast petroleum exploration from paleoecology and related stratigraphy. *Gulf Coast Association of Geological Societies Transactions*, **16**, 119–130.

Trevino, R.H., Loucks, R.G., Gale, J.F.W. and Abdelmoniem, A.K. 2007. Extending facies interpretations by integrating core, image-log, and wireline-log data in the Upper Cretaceous Olmos Formation of South

Texas. *Gulf Coast Association of Geological Societies Transactions*, **57**, 729–736.

Tyler, N. and Ambrose, W.A. 1986. *Depositional Systems and Oil and Gas Plays in the Cretaceous Olmos Formation, South Texas*. Bureau of Economic Geology Report of Investigations **152**.

Upchurch, G.R., Jr, Otto-Bliesner, B.L. and Scotese, C.R. 1999. Terrestrial vegetation and its effects on climate during the latest Cretaceous. *Geological Society of America Special Papers*, **332**, 407–426, https://doi.org/10.1130/0-8137-2332-9.407

Van Avendonk, H.J.A., Christeson, G.L., Norton, I.O. and Eddy, D.R. 2015. Continental rifting and sediment infill in the northwestern Gulf of Mexico, *Geology*, **43**, 631–634, https://doi.org/10.1130/G36798.1

Wade, B.S., Pearson, P.N., Berggren, W.A. and Pälike, H. 2011. Review and revision of Cenozoic tropical planktonic foraminiferal biostratigraphy and calibration to the geomagnetic polarity and astronomical time scale. *Earth-Science Reviews*, **104**, 111–142, https://doi.org/10.1016/j.earscirev.2010.09.003

Waltrip, N.W. 2020. *Evaluation of Regional Trends in Production for Olmos and Lower Wilcox Lobo Trends, Onshore South Texas, USA*. Masters thesis, The University of Texas at Austin.

Ward, W., Keller, G., Stinnesbeck, W. and Adatte, T. 1995. Yucatan subsurface revisited: implications and constraints for the Chicxulub meteor impact. *Geology*, **23**, 873–876, https://doi.org/10.1130/0091-7613(1995)023%3C0873:YNSSIA%3E2.3.CO;2

Weil, A.B. and Yonkee, W.A. 2012. Layer-parallel shortening across the Sevier fold-thrust belt and Laramide foreland of Wyoming: spatial and temporal evolution of a complex geodynamic system. *Earth and Planetary Science Letters*, **357**, 405–420, https://doi.org/10.1016/j.epsl.2012.09.021

Weimer, P., Bouroullec, R., Matt, V., Adson, J., van den Berg, A.A., Lapinski, T.G. and Roesink, J.G. 2016. Petroleum geology of the Mississippi Canyon, Atwater Valley, western DeSoto Canyon, and western Lloyd protraction areas, northern deepwater Gulf of Mexico: Seals, sourcerocks, generation, and accumulation: preliminary results. *Gulf Coast Association of Geological Societies Transactions*, **66**, 601–624.

Weise, B.R. 1980. *Wave-Dominated Delta Systems of the Upper Cretaceous San Miguel Formation, Maverick Basin, South Texas*. The University of Texas at Austin, Bureau of Economic Geology. Report of Investigations **107**, https://www.beg.utexas.edu/publications/wave-dominated-delta-systems-upper-cretaceous-san-miguel-formation-maverick-basin

Witts, J.D., Landman, N.H. *et al*. 2018. A fossiliferous spherule-rich bed at the Cretaceous–Paleogene (K–Pg) boundary in Mississippi, USA: implications for the K/Pg mass extinction event in the Mississippi embayment and eastern Gulf Coastal Plain. *Cretaceous Research*, **91**, 147–167, https://doi.org/10.1016/j.cretres.2018.06.002

Xaio, L., Zhao, J.W. *et al*. 2017. Ages and geochemistry of the basement granites of the Chicxulub impact crater: implications for peak ring formation. *Lunar and Planetary Science*, **48**, 1–2, https://www.hou.usra.edu/meetings/lpsc2017/pdf/1311.pdf

Yancey, T.E. and Liu, C. 2013. Impact-induced sediment deposition on an offshore, mud substrate continental shelf, Cretaceous–Paleogene boundary Brazos River, Texas, USA. *Journal of Sedimentary Research*, **83**, 354–367, https://doi.org/10.2110/jsr.2013.30